NEW Fluctuation and Low-p_T Correlation Results from PHENIX

Workshop on Correlations and Fluctuations in Relativistic Nuclear Collisions – 7/8/06

Jeffery T. Mitchell

(Brookhaven National Laboratory)

Outline

- **Multiplicity Fluctuations**
- **Correlation Lengths**

  (using multiplicity fluctuations)
- **Low-p_T Correlations**

The PHENIX Detector

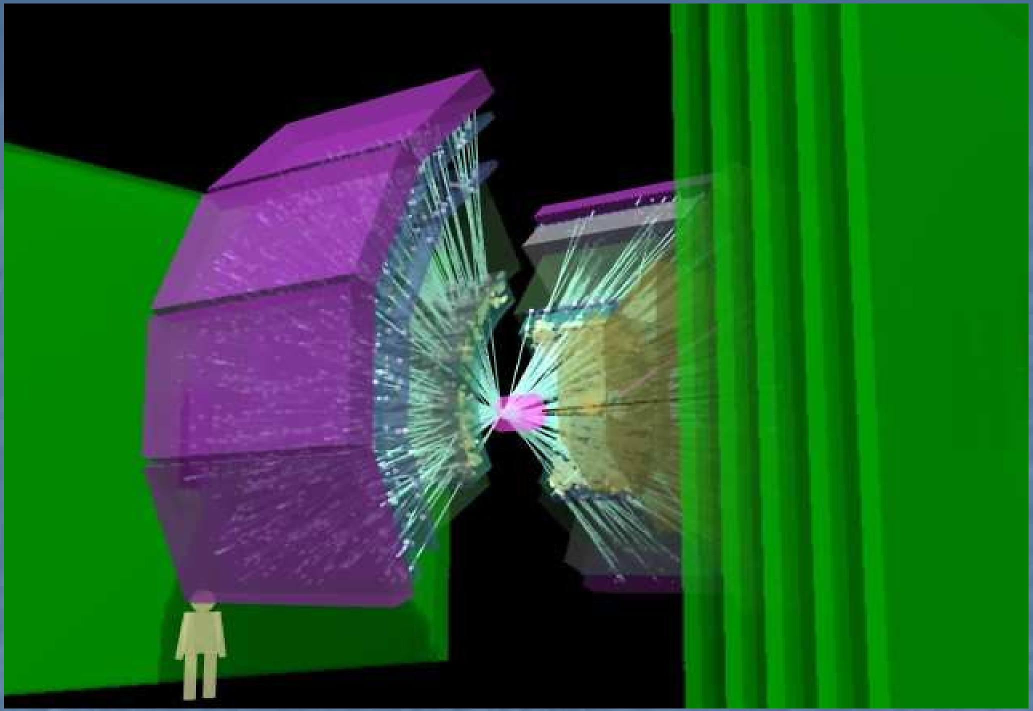

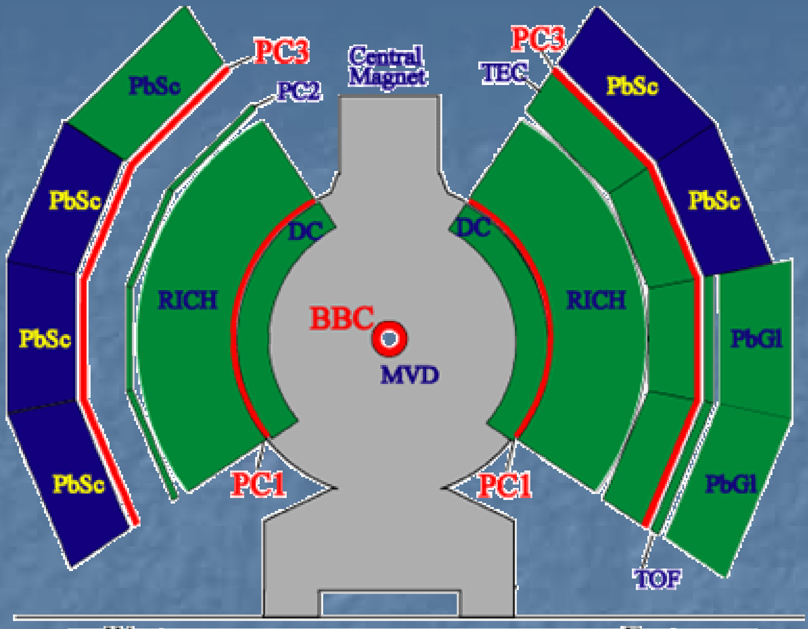

Acceptance:

$|\eta| \sim 0.35$, $|\Delta\phi| \sim \pi$

Two "central arm" spectrometers anchored by drift chambers and pad chambers for 3-D track reconstruction within a focusing magnetic field.

Although the PHENIX acceptance is traditionally considered small for event-by-event measurements, the acceptance is large enough to provide a competitive sensitivity to most observables.

Measuring Multiplicity Fluctuations with Negative Binomial Distributions

Multiplicity distributions in hadronic and nuclear collisions can be described by the Negative Binomial Distribution. The magnitude of the parameter k describes the deviation from a Poisson distribution → higher k means more Poissonian.

UA5: sqrt(s)=546 GeV p-pbar, Phys. Rep. 154 (1987) 247.

E802: 14.6A GeV/c O+Cu, Phys. Rev. C52 (1995) 2663.

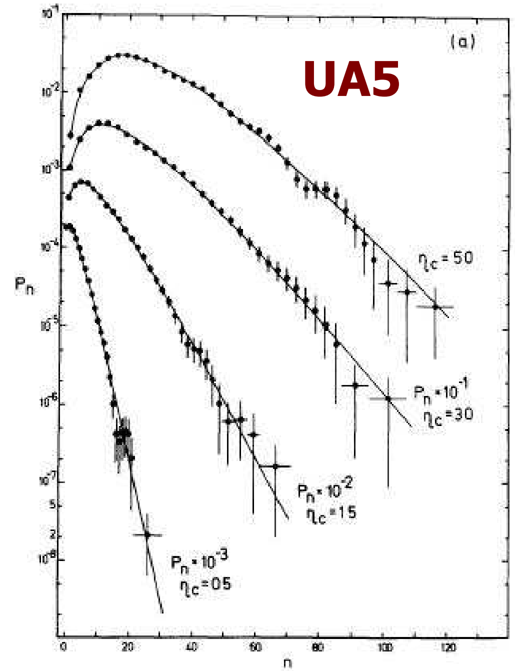

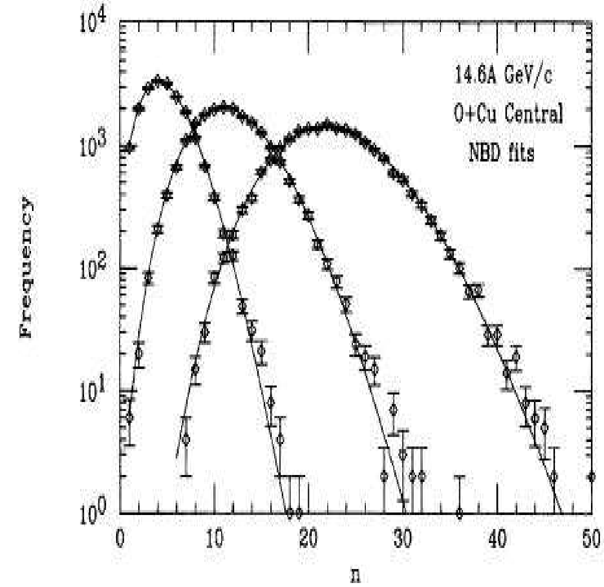

E802

PHENIX Preliminary, 62 GeV Au+Au

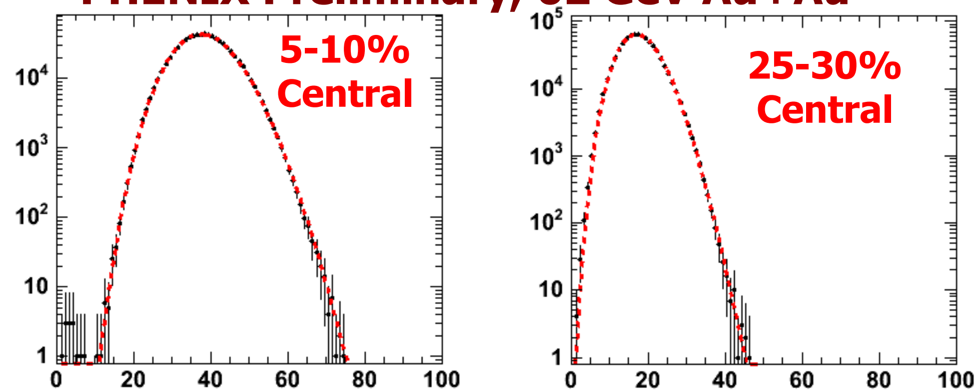

$$P(m) = \frac{(m+k-1)!}{m!(k-1)!} \frac{\left(\mu/k\right)^m}{\left(1+\mu/k\right)^{m+k}}$$

$$\frac{1}{k} = \frac{\sigma^2}{\mu^2} - \frac{1}{\mu}$$

Impact Parameter Fluctuations: Data

A major source of non-dynamical fluctuations are contributions due to geometry (N_{part}) fluctuations due to the finite width of the centrality bin. This can be demonstrated directly with data…

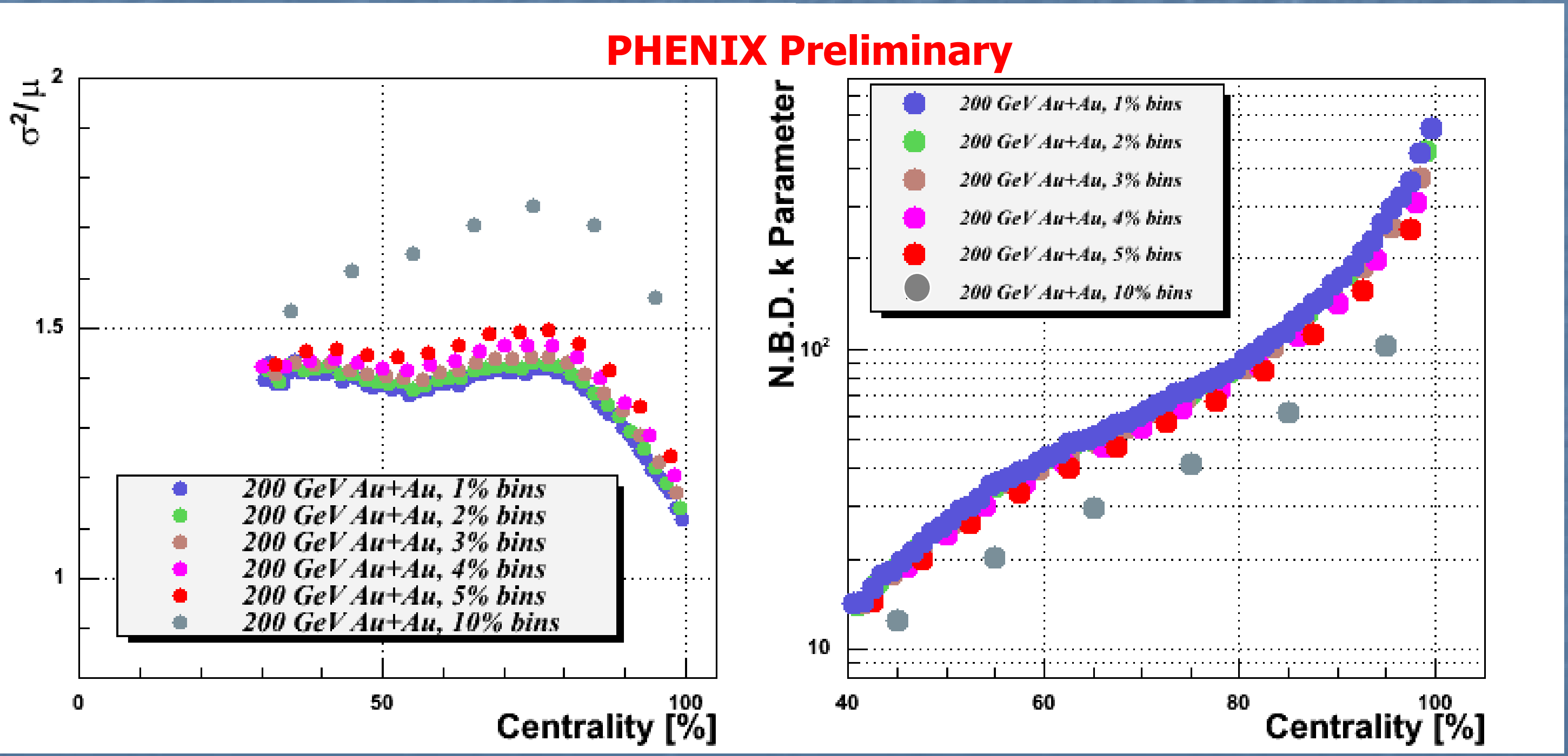

Geometry fluctuations drive σ^2/μ down and N.B.D. k up.

Impact Parameter Fluctuations: Estimation Using HIJING 1.37

Corrections for geometry fluctuations are estimated using HIJING 1.37 run a) with a fixed impact parameter, and b) with an impact parameter covering the range of the 5% centrality bin. Estimations match the 1% centrality data. Estimated systematic errors are 12-15% (included in all further data points.

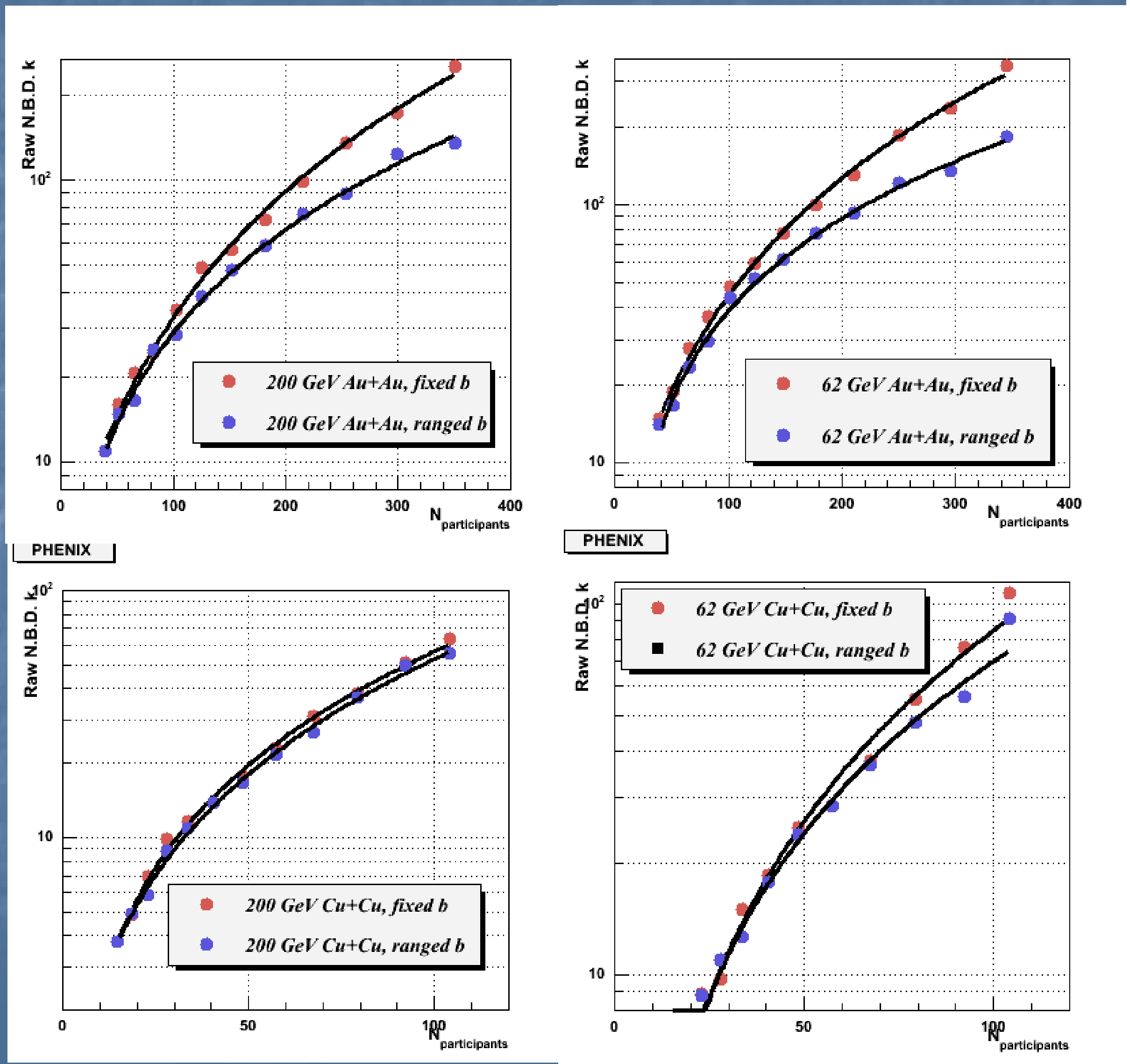

A Survey of Scaled Variance, σ^2/μ

- Inclusive charged hadron fluctuations.
- $0.2 < p_T < p_{T,max}$ GeV/c
- These values are corrected to remove the contribution due to impact parameter (geometrical) fluctuations and projected to 2π in azimuth for direct comparisons to NA49 and other experiments.
- The Poissonian (random) limit is 1.0.
- Large non-random fluctuations are observed that increase with p_T and decrease with centrality, although the p_T-dependence is relatively weak, unlike $<p_T>$ fluctuations.

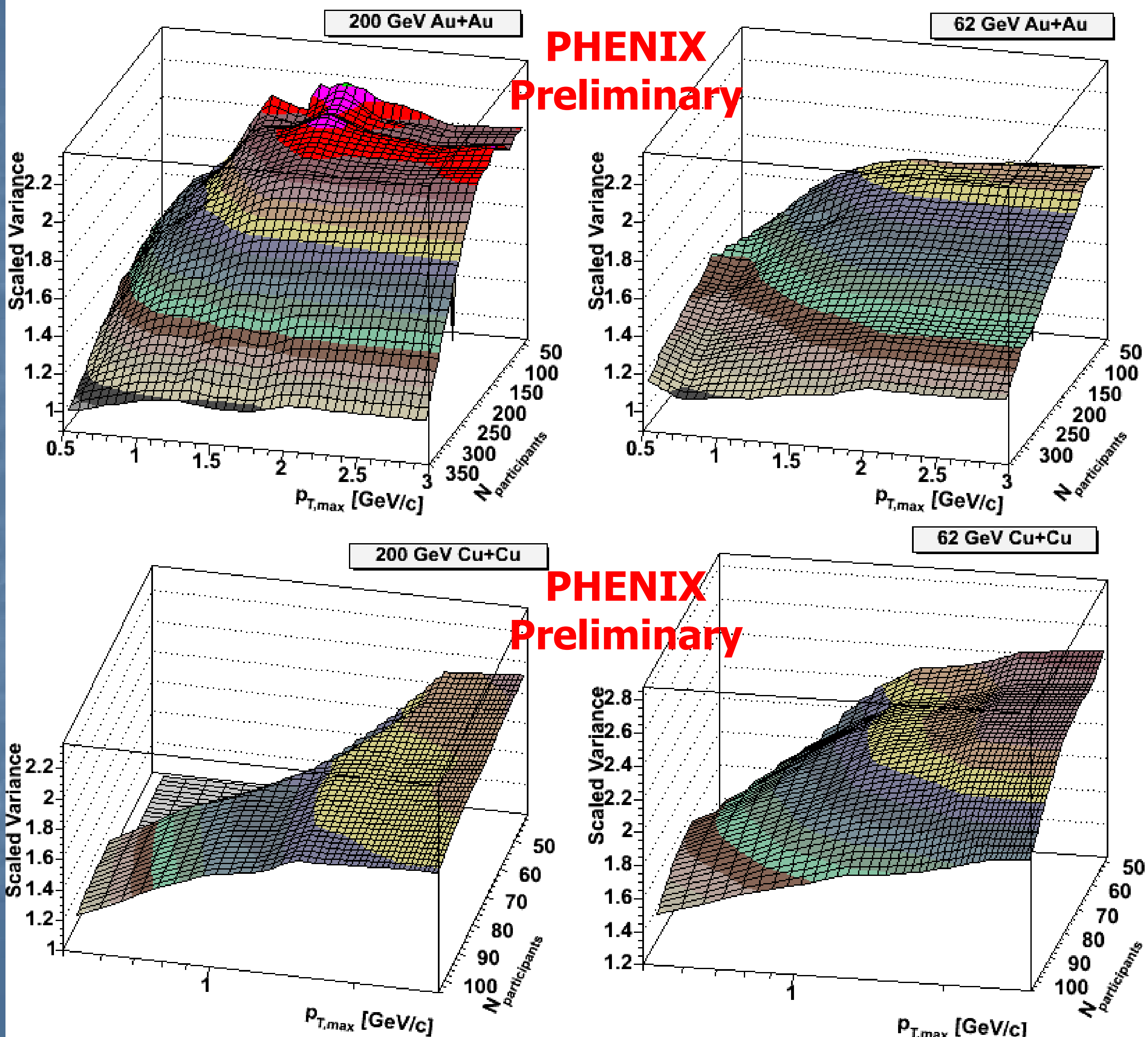

Fluctuations over the entire p_T range

$0.2 < p_T < 3.0$ GeV/c

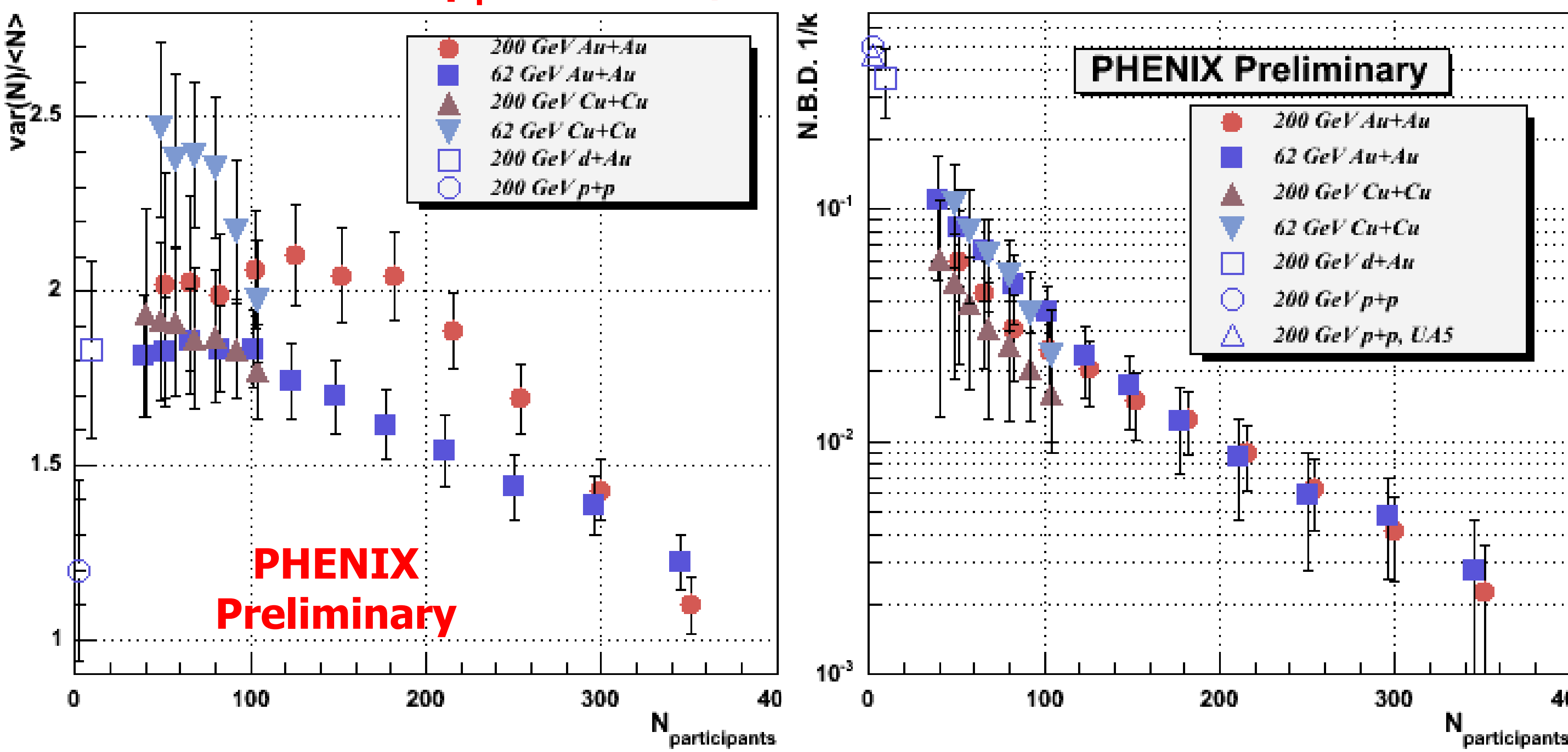

Inclusive charged hadron fluctuations. All points are projected to 2π azimuthal acceptance, corrected for detector occupancy and efficiency. All points are corrected for non-dynamical geometry fluctuations due to the finite width of the centrality bins. Errors include time-dependent systematic errors, azimuthal extrapolation systematic errors, and impact parameter correction systematic errors. p+p fluctuations are consistent with projections of UA5 results to sqrt(s)=200 GeV.

Thermodynamically Motivated Observables: Relating distributions to compressibility

- In the Grand Canonical Ensemble, the variance in particle number N (with μ=<N>) is related to the compressibility, k_T, via

$$\sigma^2 / \mu = \frac{k_B T \mu}{V} k_T$$

- The N.B.D. k parameter is related to the scaled variance via

$$\sigma^2 / \mu = 1 + \mu / k_{NBD}$$

- N.B.D. k can then be related to compressibility:

$$1 / k_{NBD} = \frac{k_B T}{V} k_T - 1 / \mu$$

Multiplicity Fluctuations: Universal Scaling

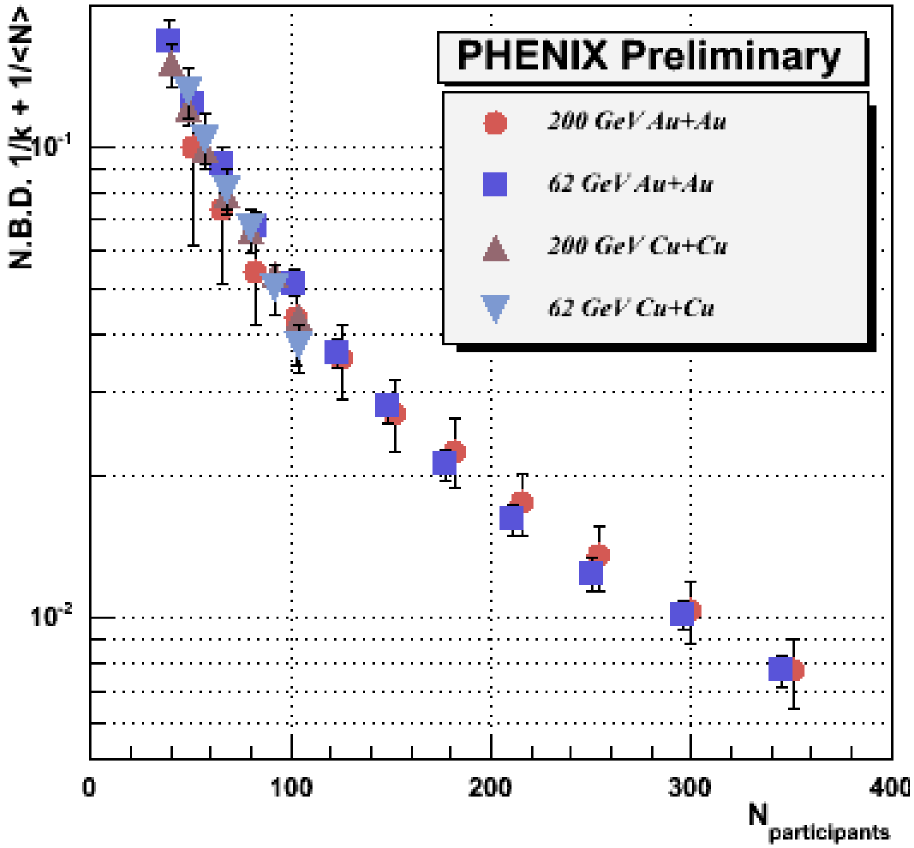

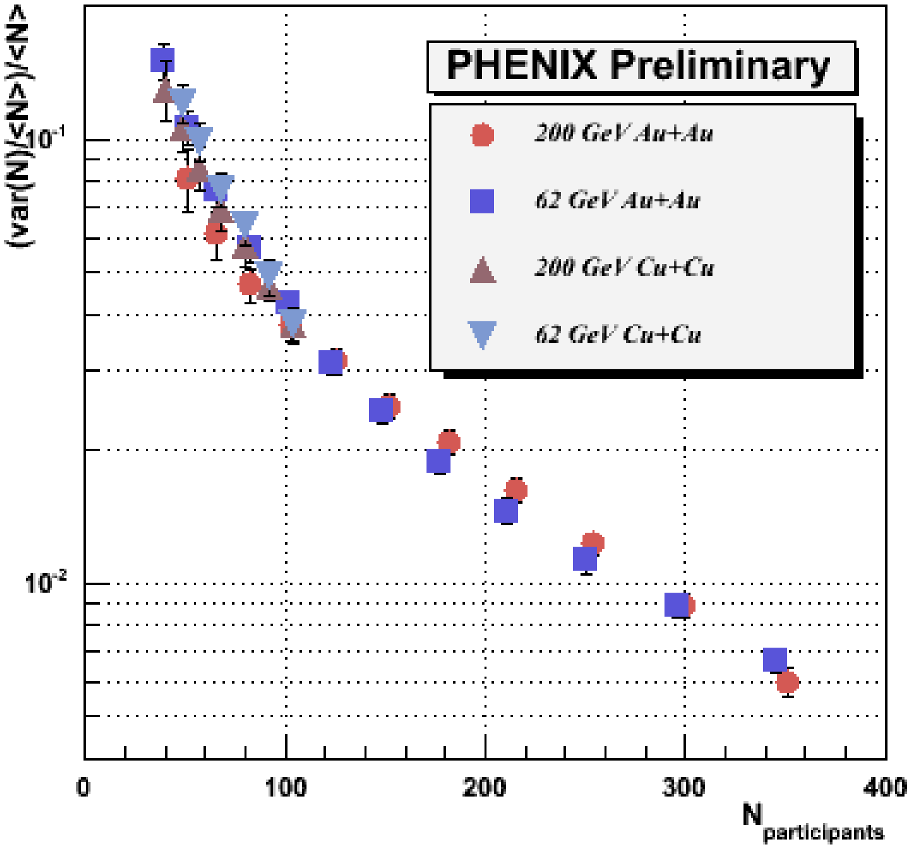

All species scaled to the 200 GeV dataset.
The data appear to follow a universal curve.

This curve is a power law function.

Multiplicity Fluctuations: Universal Scaling

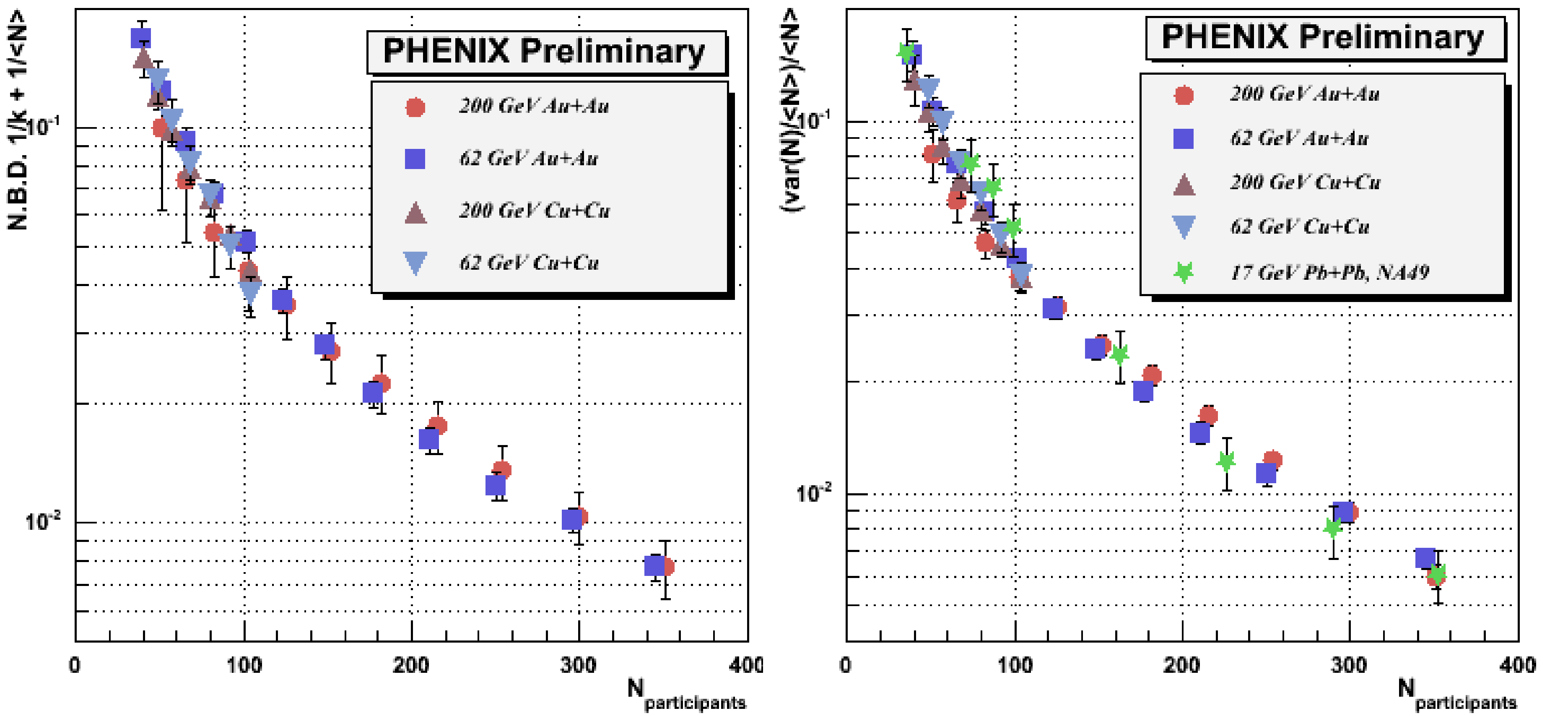

NA49 data corrected for geometry fluctuations (10% centrality bins) also lie on the universal curve.

Multiplicity Fluctuations: Universal Scaling

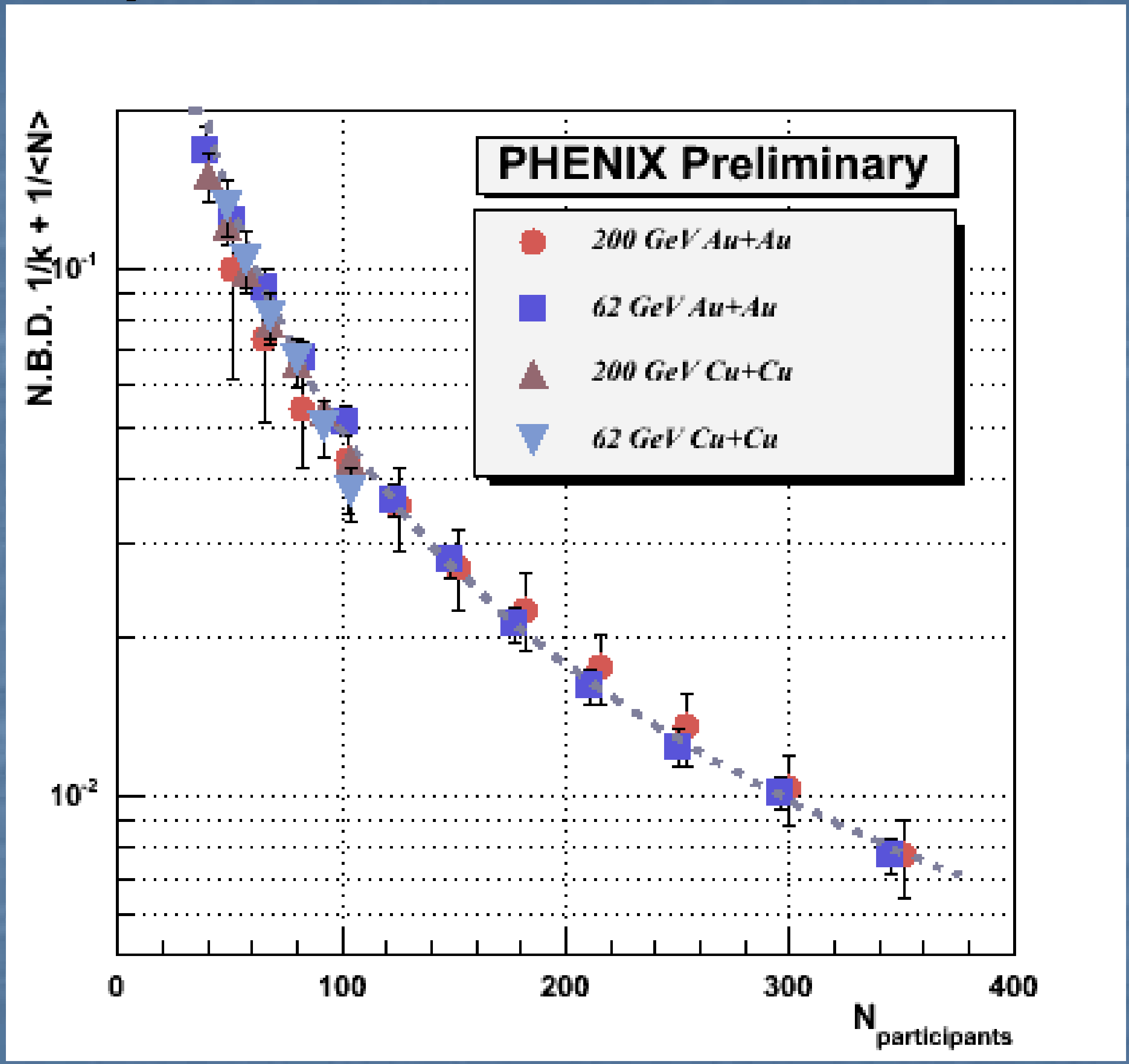

The universal curve can be described by a power law function of N_{part}.

Multiplicity Fluctuations: Extracting a Correlation Length

- **The correlation length, ξ , is expected to diverge at the critical point.**
- **To extract ξ, the N.B.D. k parameter is extracted by fitting the multiplicity distribution in successive ranges of $\delta\eta$ or $\delta\phi$.**
- **NBD k can be related to a correlation length as follows (see *E802, Phys. Rev. C52 (1995) 2663* and K. Homma's presentation):**

$$\frac{1}{k} = \frac{2\alpha\xi^2\left(\frac{\delta\eta}{\xi} - 1 + e^{-\frac{\delta\eta}{\xi}}\right)}{\delta\eta^2} + \beta$$

Here, α is fixed to 0.5 (based on PHENIX preliminary correlation function measurements). β and ξ are free parameters.

Example: N.B.D. k vs. dη

$$\frac{1}{k(\delta\eta)} = \frac{2\alpha\xi^2(\delta\eta/\xi - 1 + e^{-\delta\eta/\xi})}{\delta\eta^2} + \beta$$

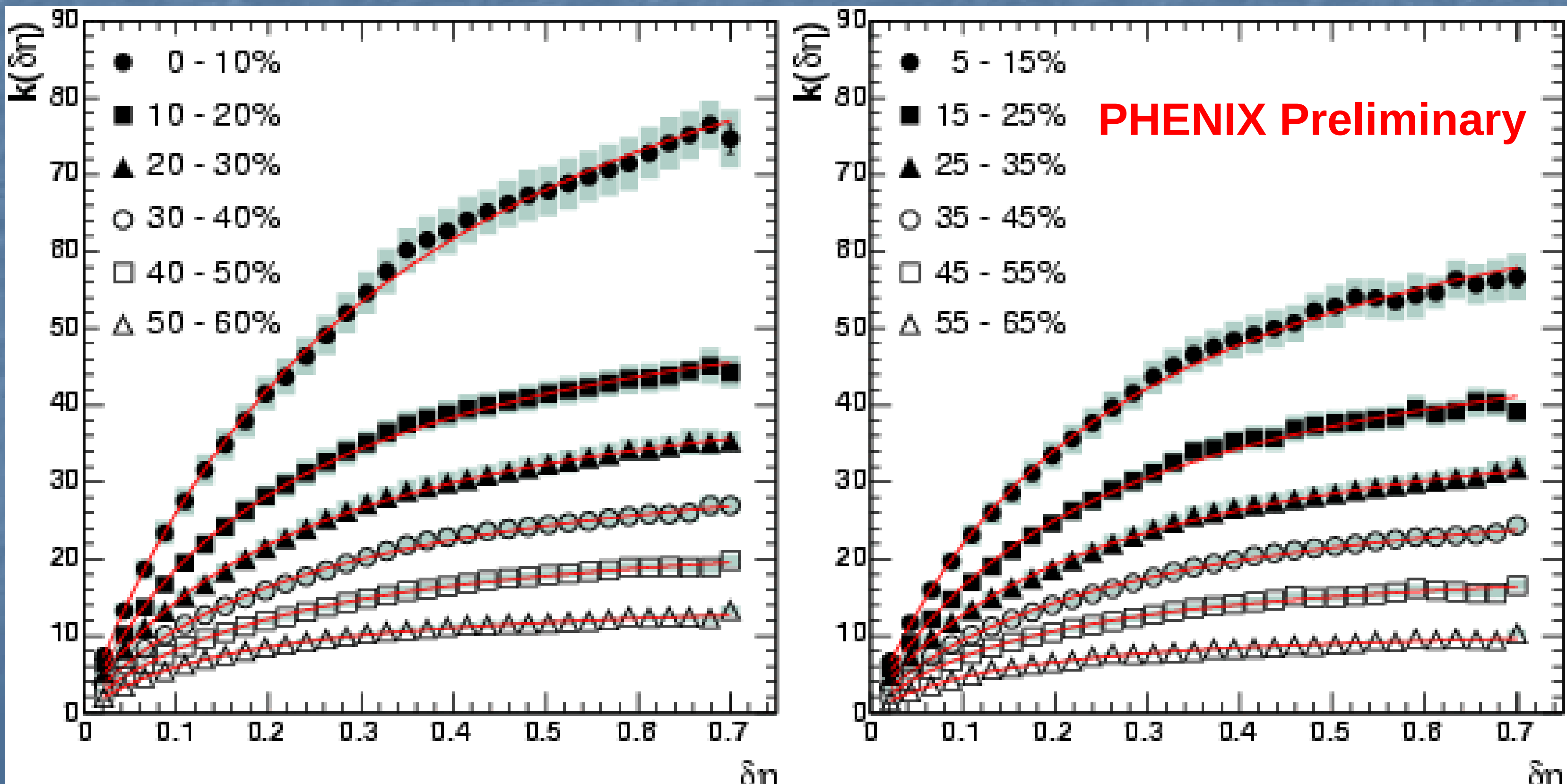

Correlation length ξ and static susceptibility χ

Divergence of correlation length is the indication of a critical temperature.

$$\xi(T) \equiv \sqrt{\frac{A(T)}{a_0(T - T_c)}}$$

Divergence of susceptibility is the indication of 2nd order phase transition.

$$\chi_k = \frac{\partial \phi_k}{\partial h} \propto \left(\frac{\partial^2 (f - f_0)}{\partial \phi^2{}_k} \right)^{-1}$$

$$= \frac{1}{a_0(T - T_c)(1 + k^2 \xi^2)}$$

$$\chi_{k=0} = \frac{1}{a_0(T - T_c)} \propto \frac{\xi}{T} G_2(0)$$

$$\boxed{\chi_{k=0} T \propto \bar{\rho}_1^2 \alpha \xi}$$

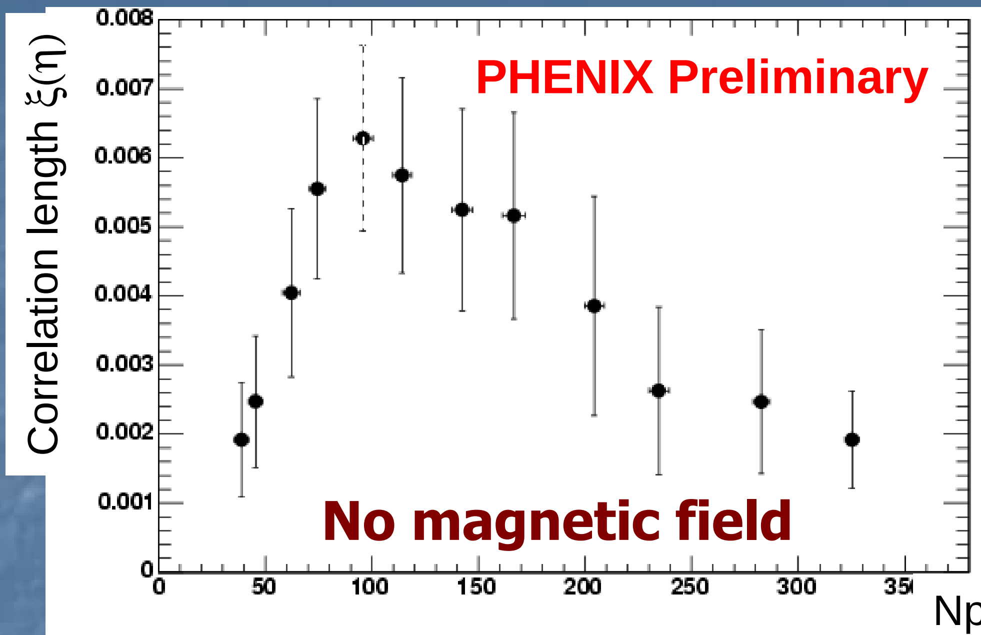

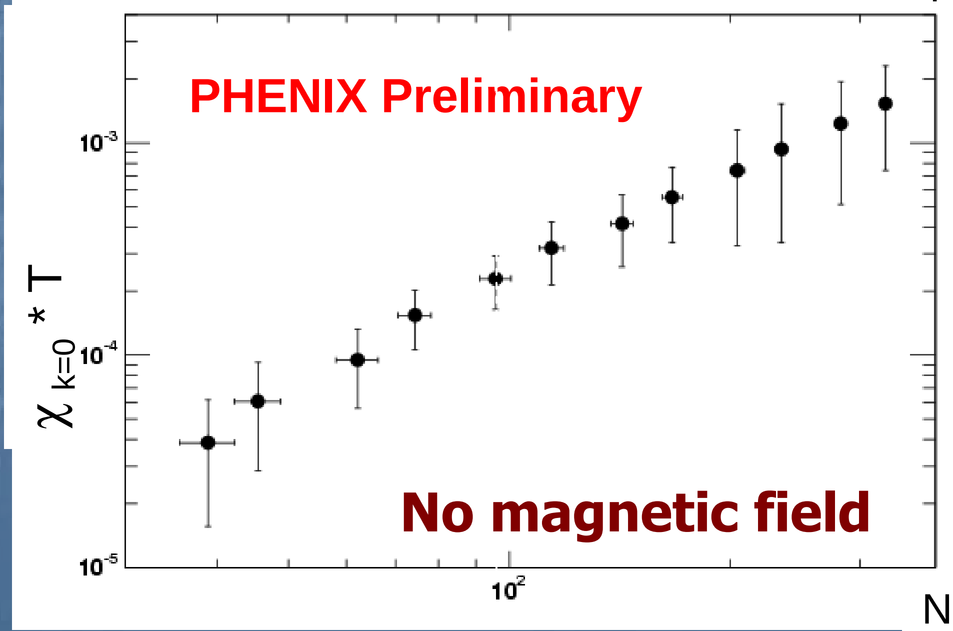

Systematic check of the correlation length

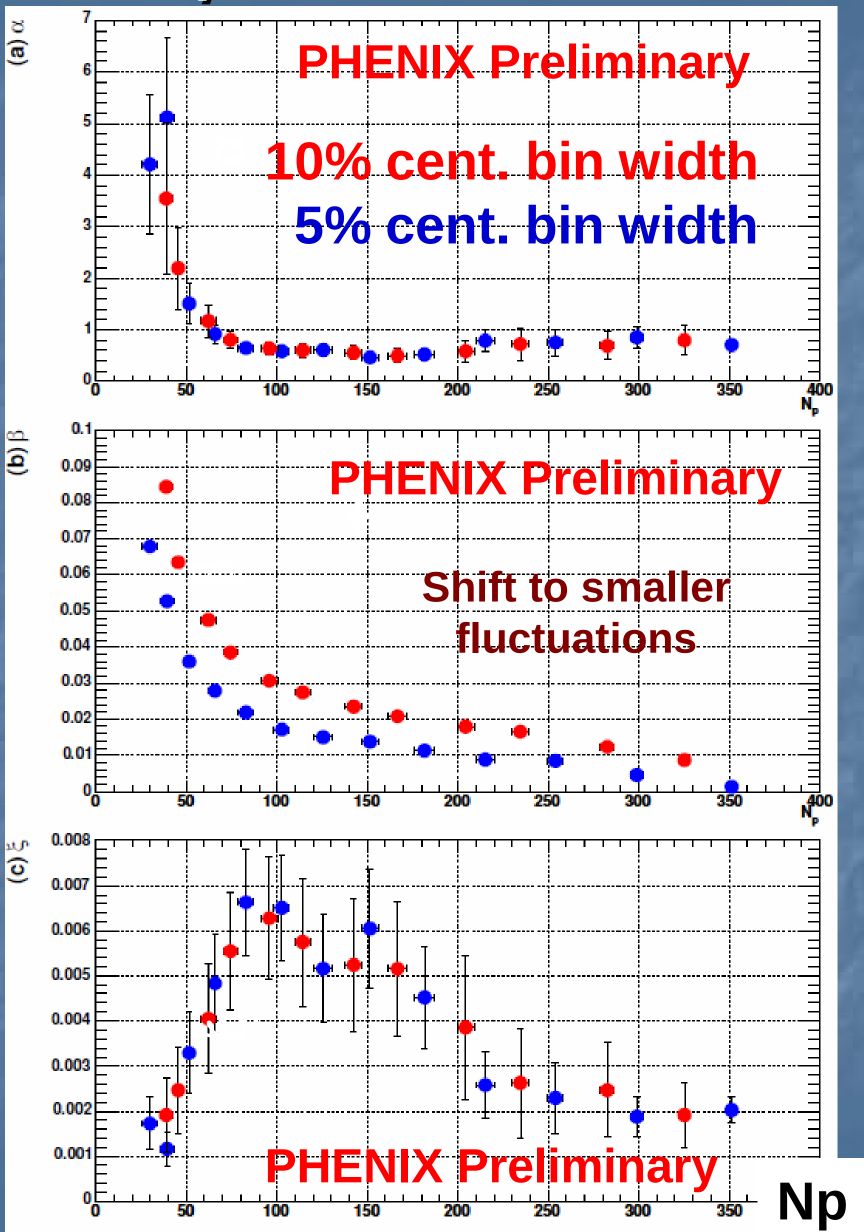

β can absorb finite centrality bin width effects, namely, finite initial temperature fluctuations, while physically important parameters are stable.

No magnetic field

Correlation length (η) in centrality and $p_{T,max}$

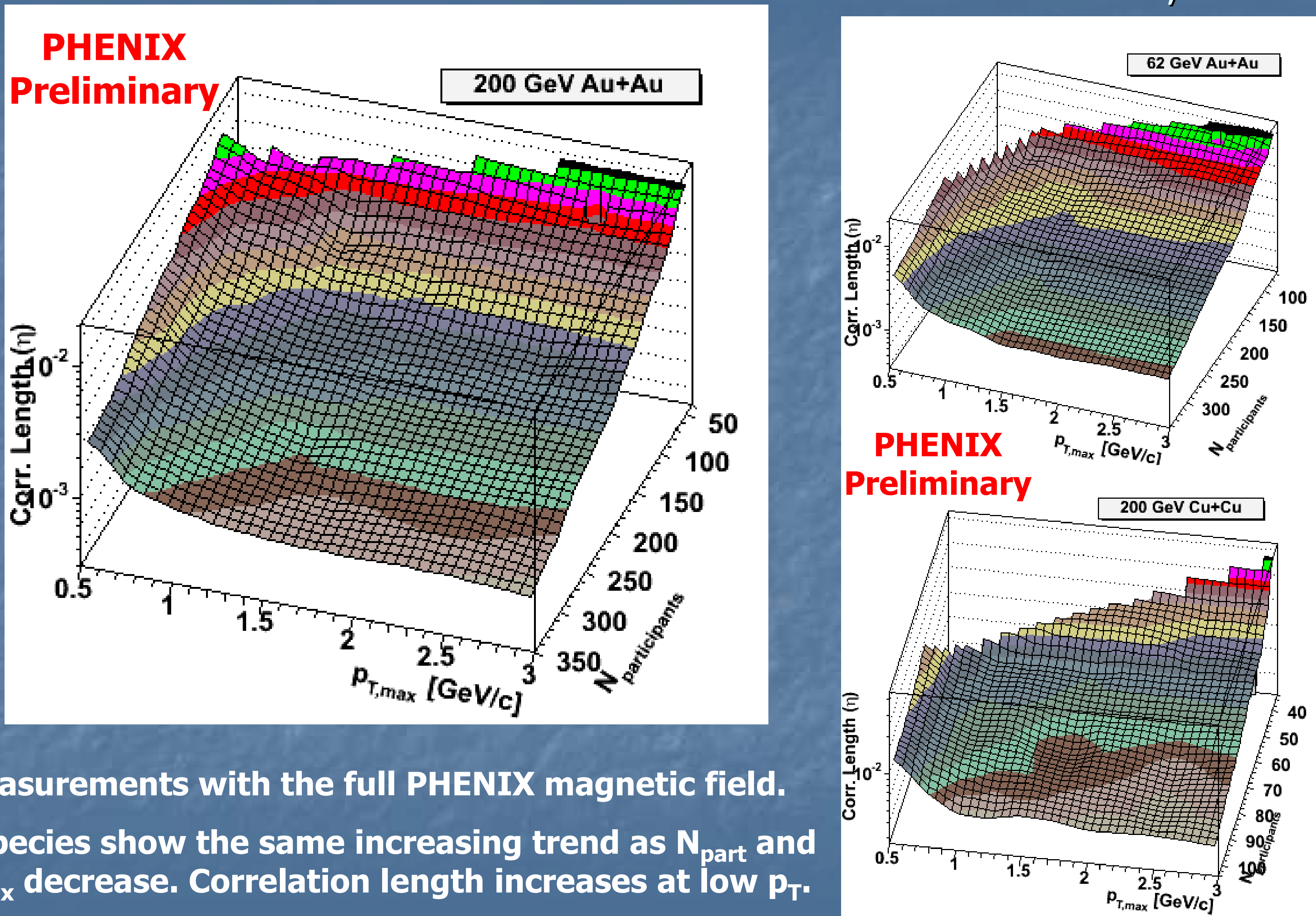

Measurements with the full PHENIX magnetic field.

All species show the same increasing trend as N_{part} and $p_{T,max}$ decrease. Correlation length increases at low p_T.

Correlation length (ϕ) in centrality and $p_{T,max}$

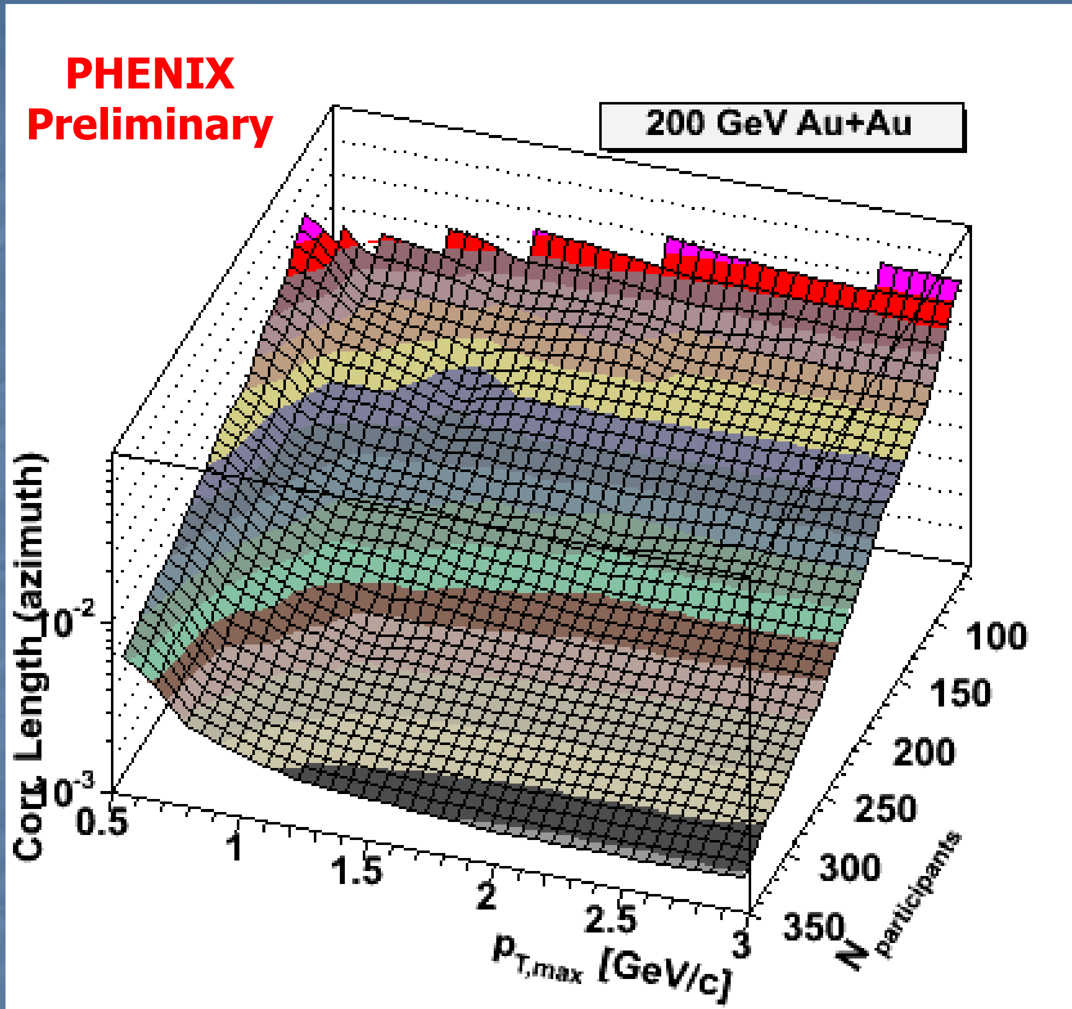

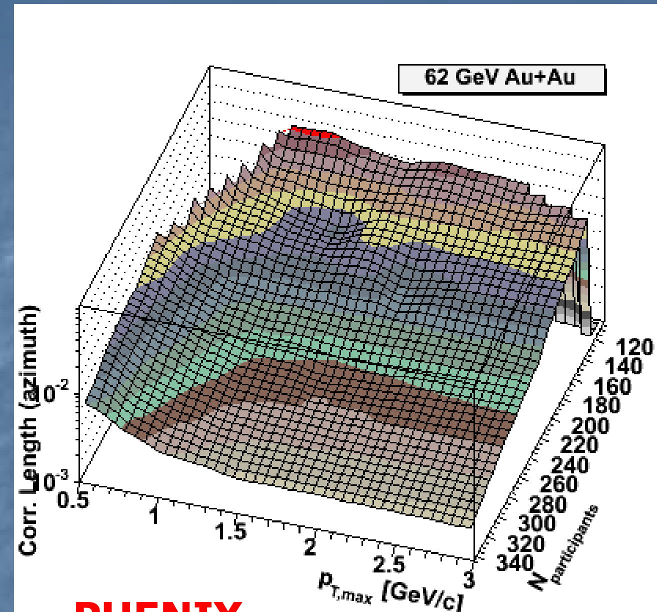

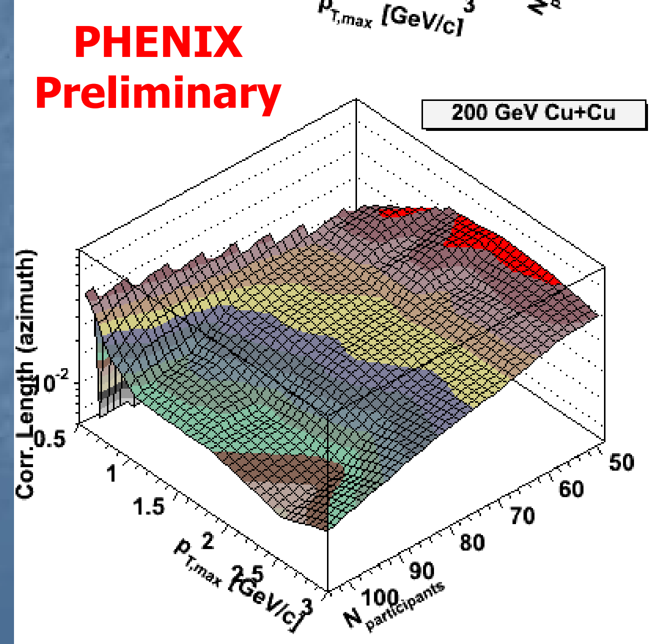

All species show the same increasing trend as N_{part} and $p_{T,max}$ decrease. Correlation length increases at low p_T.

Correlation Length vs. Centrality

0.2 < p_T < 3.0 GeV/c

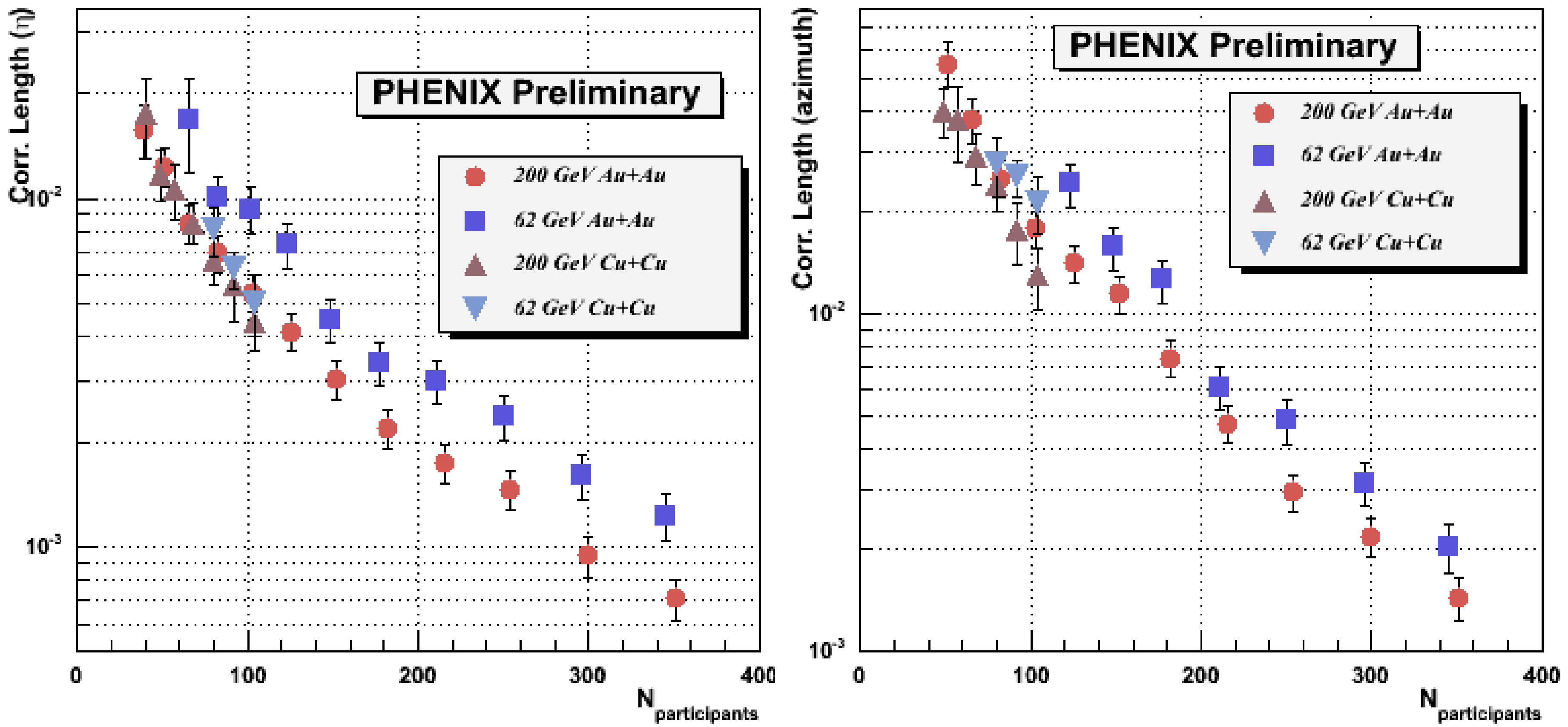

The correlation lengths are small, but cannot be explained by detector resolution effects.

Correlation lengths increase from 200 to 62 GeV.

Correlation Length vs. Centrality

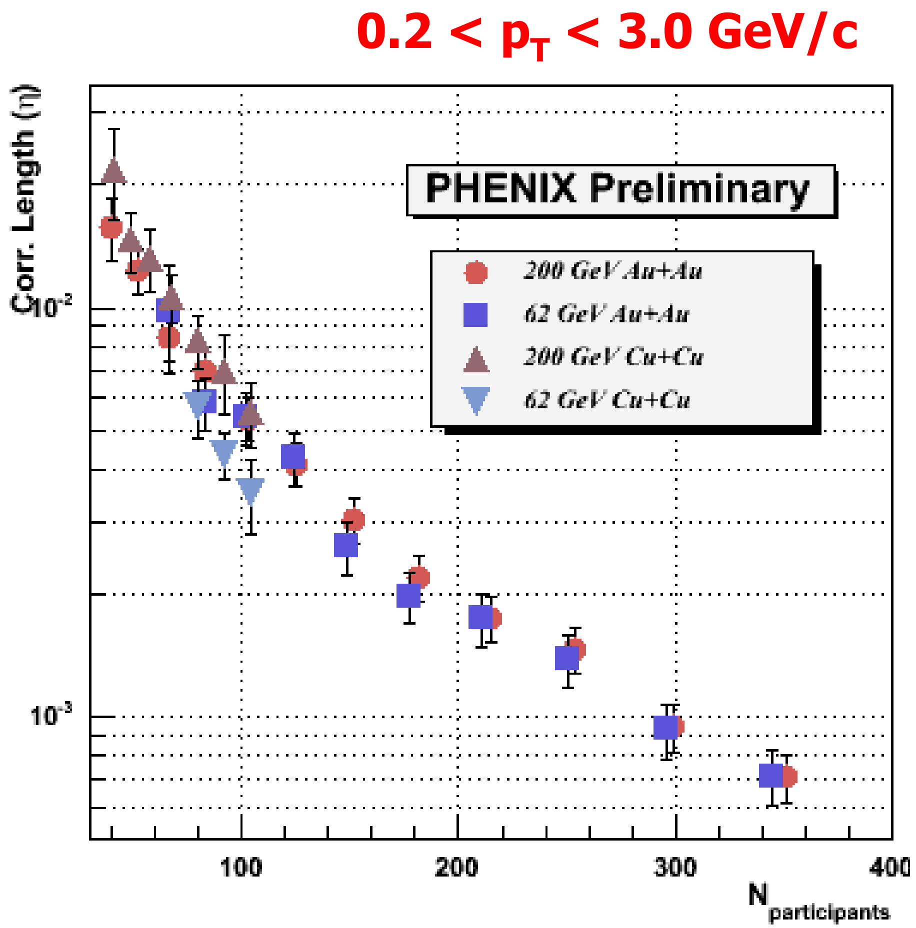

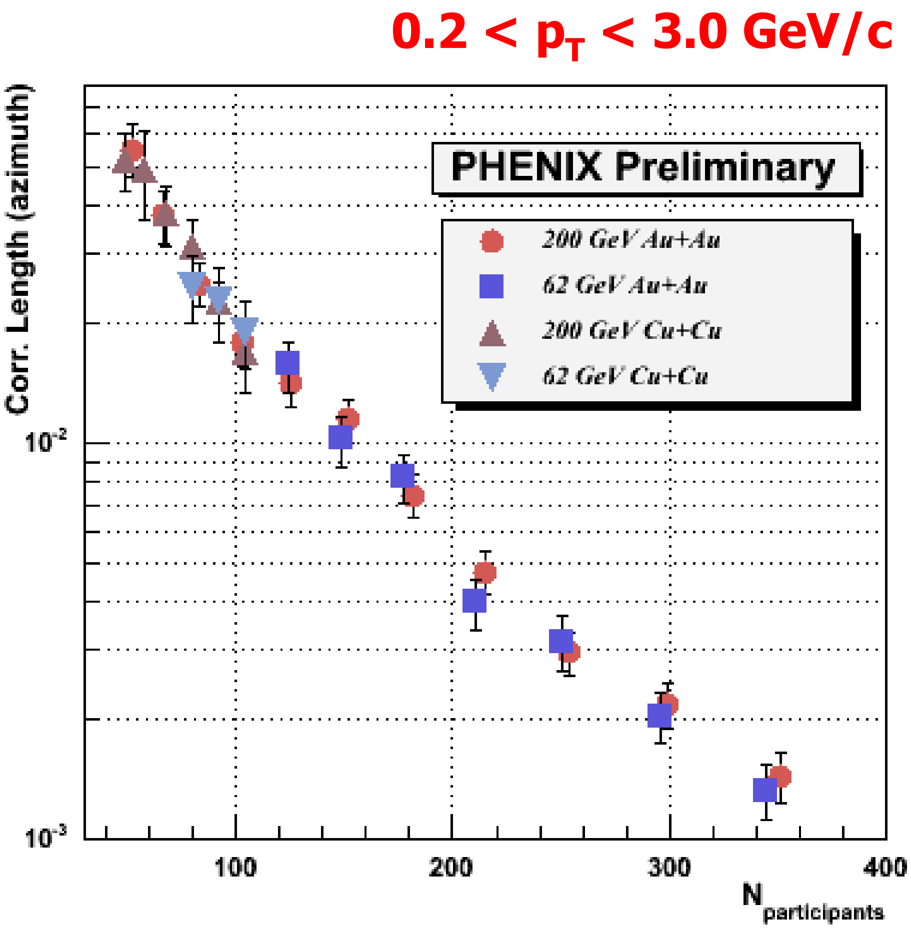

These points have been scaled to match the 200 GeV data. Notice that the correlation lengths exhibit a universal behavior as a function of centrality.

Correlation Lengths: Universal Scaling

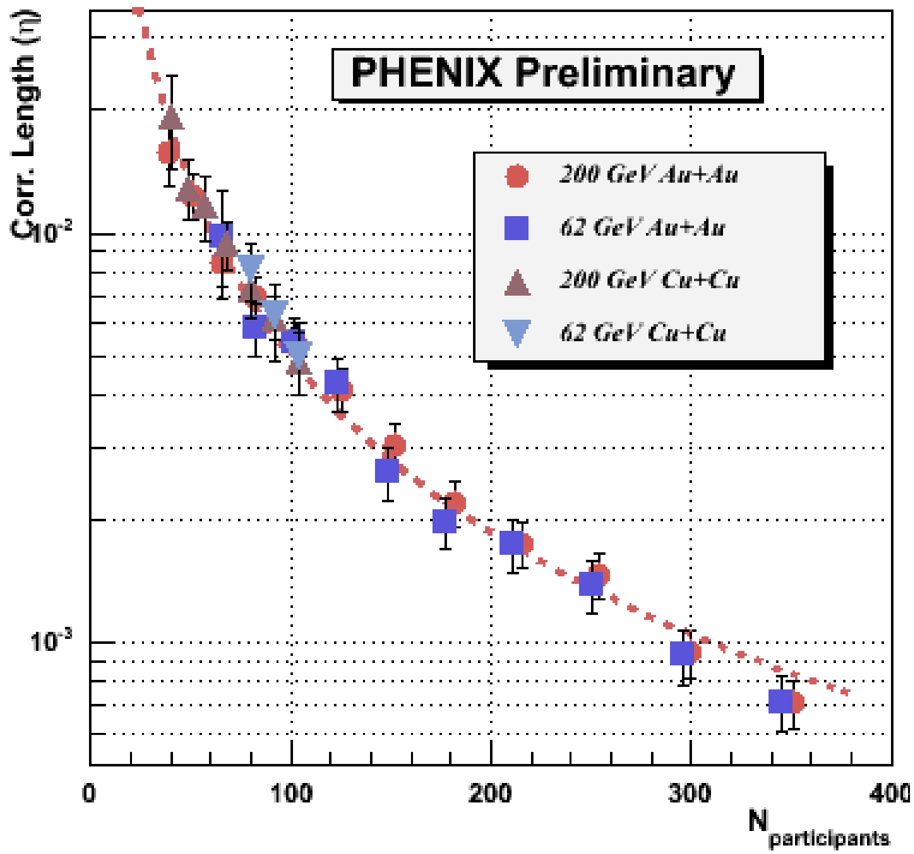

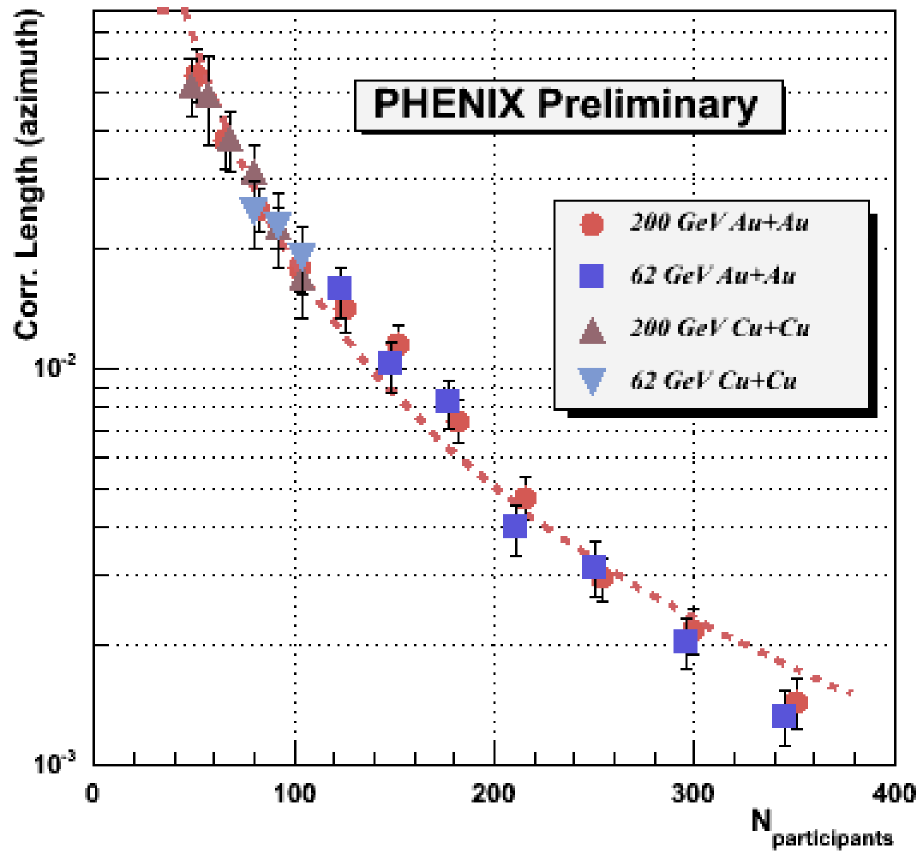

The universal curves can be described by a power law function of N_{part}.

Universal Scaling: p_T-independent

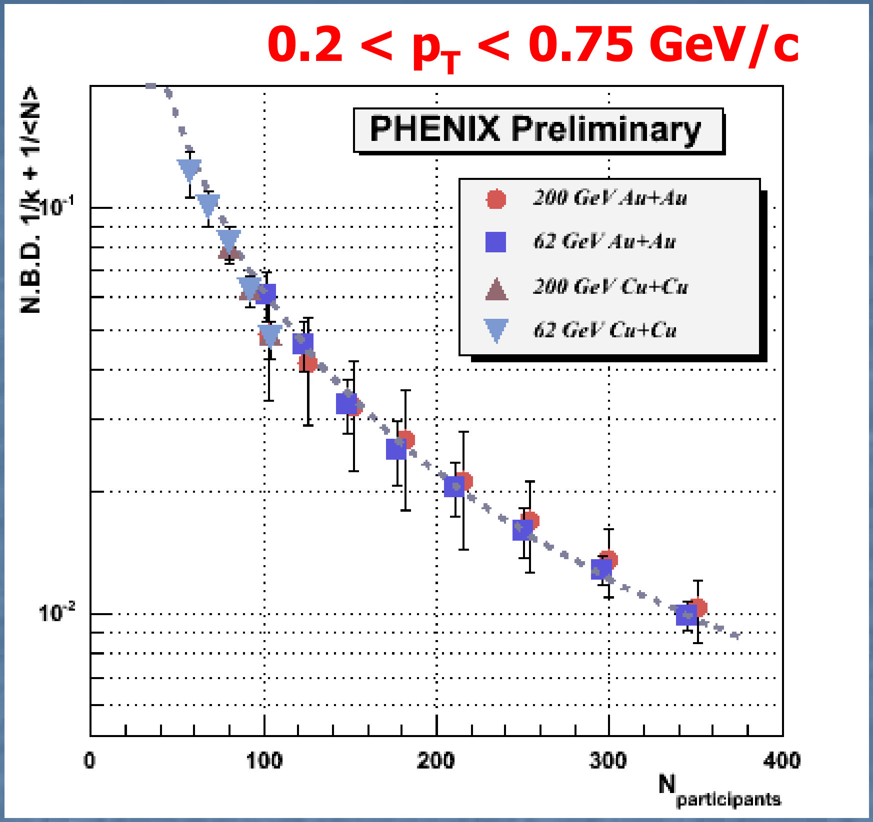

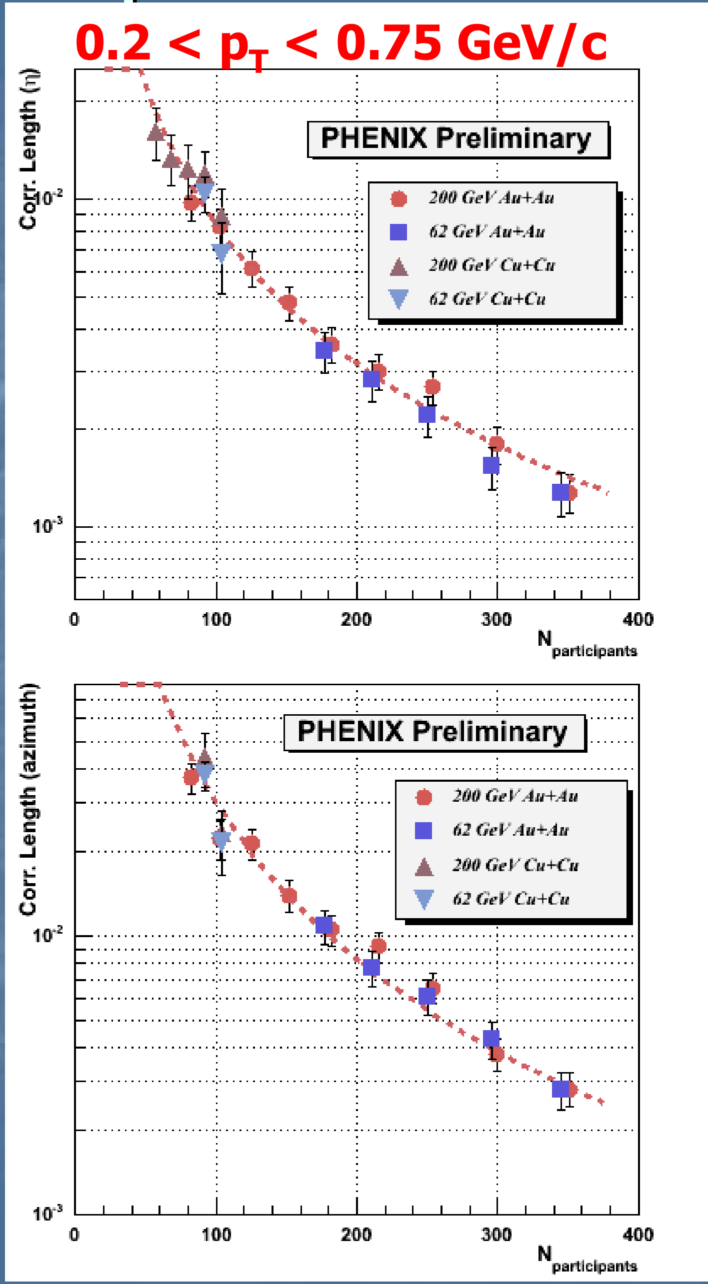

The power law curves describing the data are independent of p_T range. The scaling appears to be driven by low p_T processes.

$<p_T>$ Fluctuations

Gamma distribution calculation for statistically independent particle emission with input parameters taken from the inclusive spectra. *See M. Tannenbaum, Phys. Lett. B498 (2001) 29.*

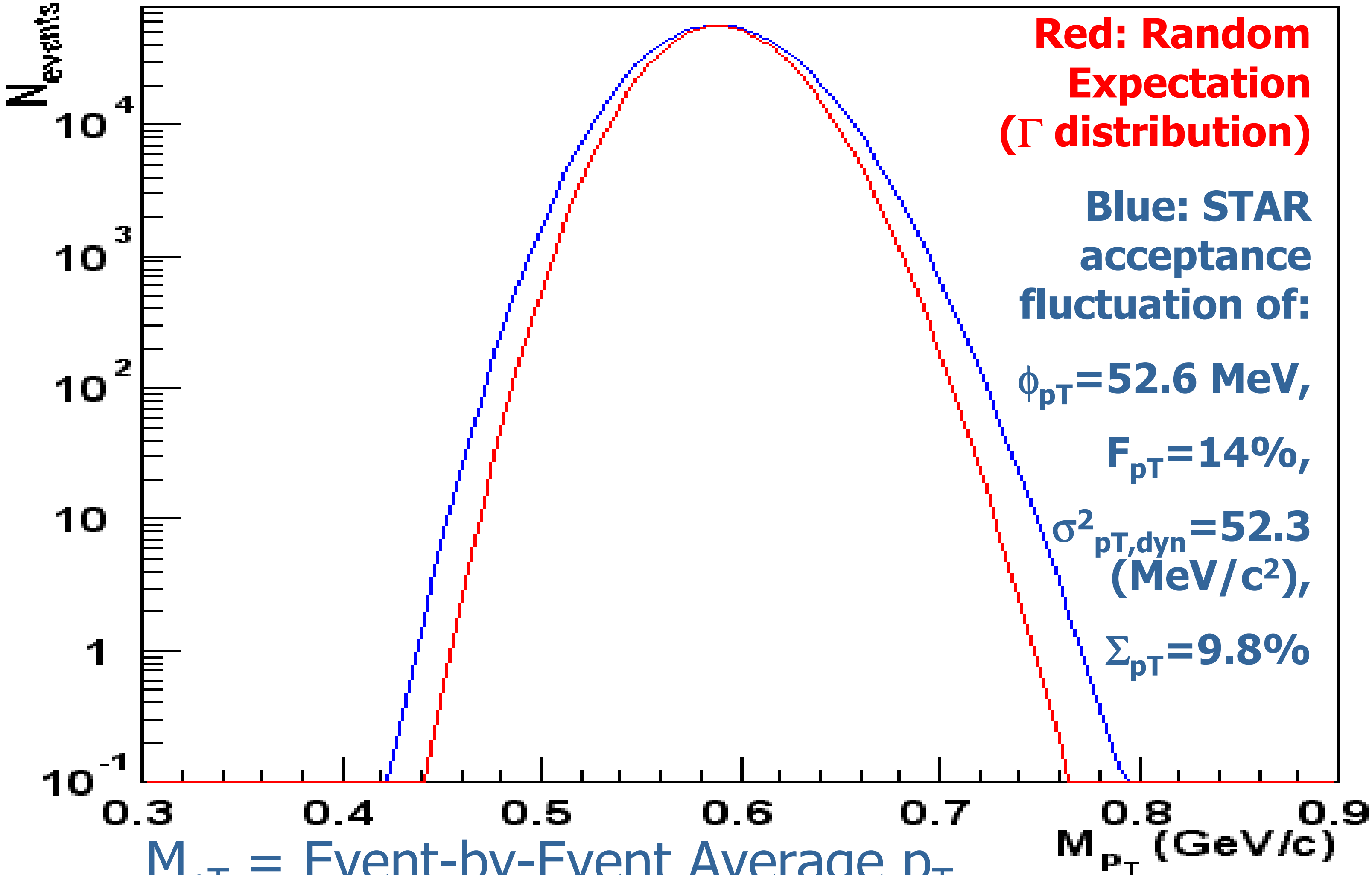

M_{pT} = Event-by-Event Average p_T

PHENIX Event-by-Event $<p_T>$ Fluctuation Results

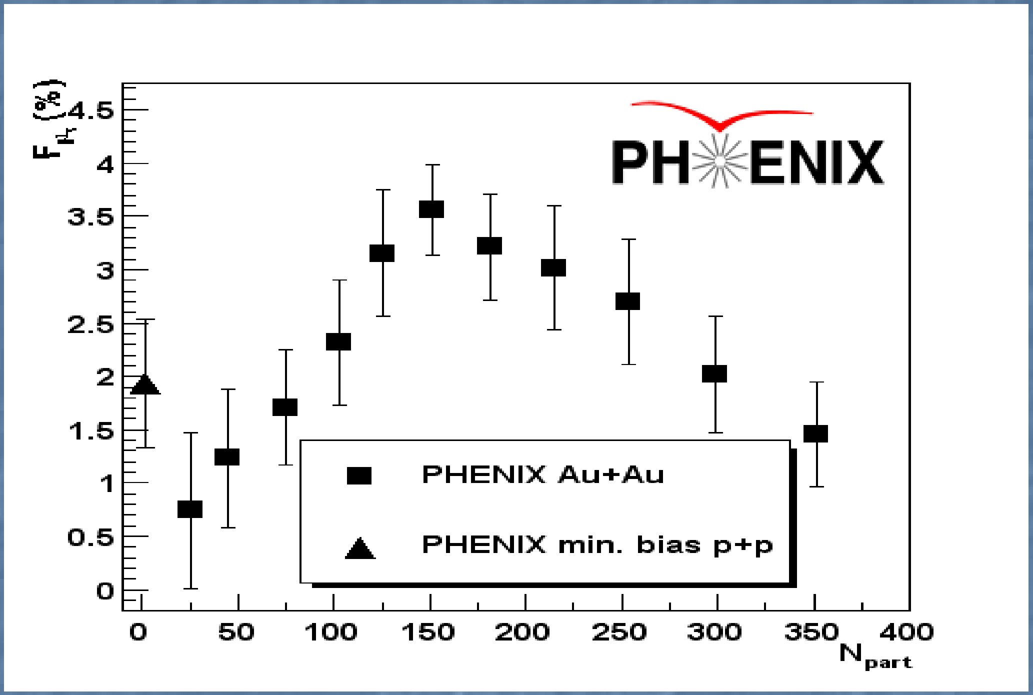

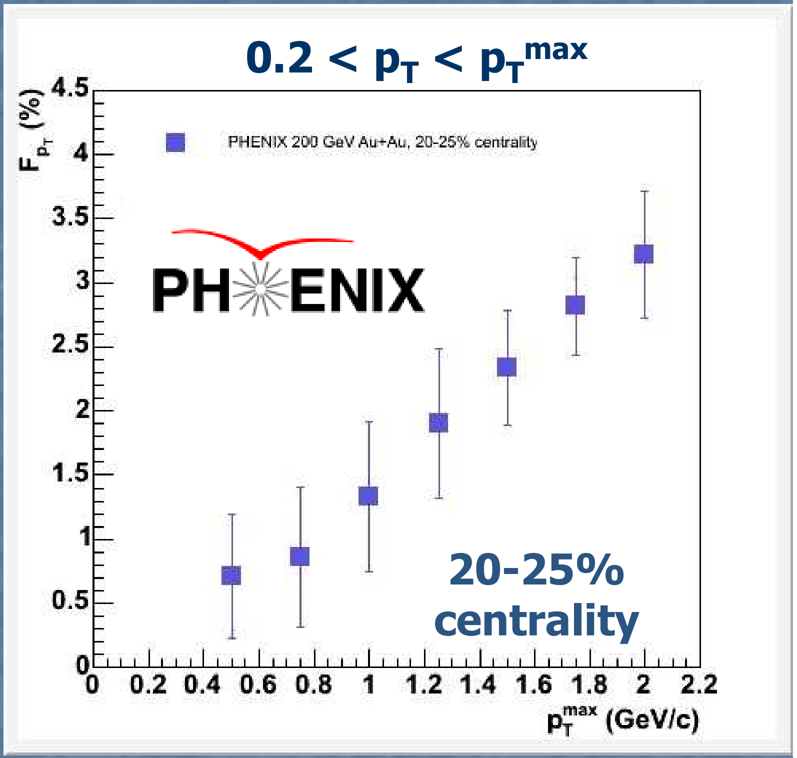

Highlights: Non-random fluctuations are observed. Non-monotonic centrality-dependence. Strong p_T-dependence. p_T fluctuations appear to be driven by high p_T particles. The shape can be explained using a PYTHIA-based simulation by the contribution of correlations due to jets.

S. Adler et al., Phys. Rev. Lett. 93 (2004) 092301.

$\langle p_T \rangle$ Fluctuations: Universal Scaling?

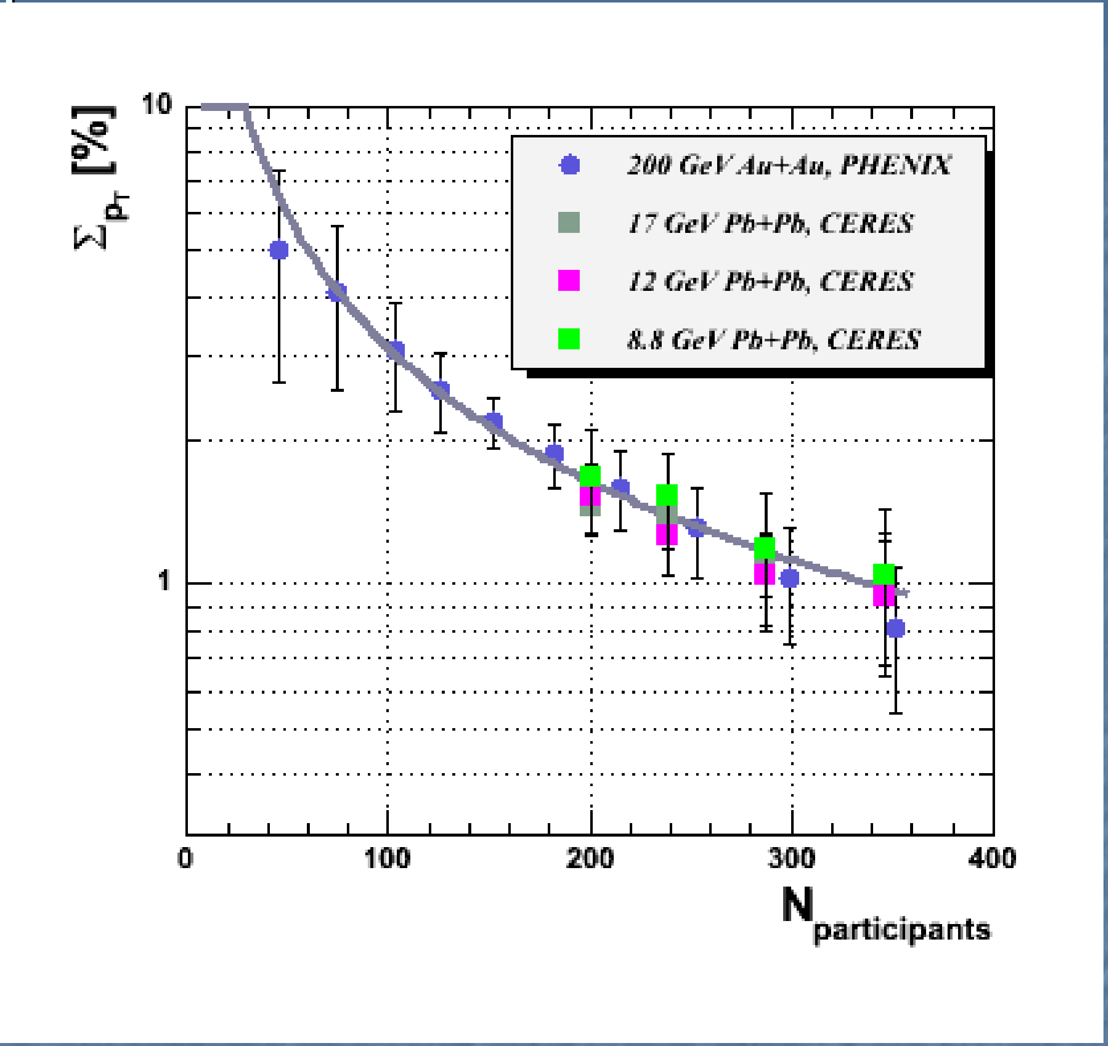

The universal curves can be described by a power law function of N_{part}, but the error bars are large.

Two-Particle Correlations at Low p_T

- **Most charged particle correlation results are performed in the interesting high-p_T region.**
- **The low-p_T region and its evolution to the high p_T region is interesting too!**
- **This study will quote correlation amplitudes in a given centrality, p_T, and $\Delta\phi$ bin determined using the mixed event method via:**

$C(\Delta\phi) = (N_{data}/N_{mixed})*(N_{events,mixed}/N_{events,data})$

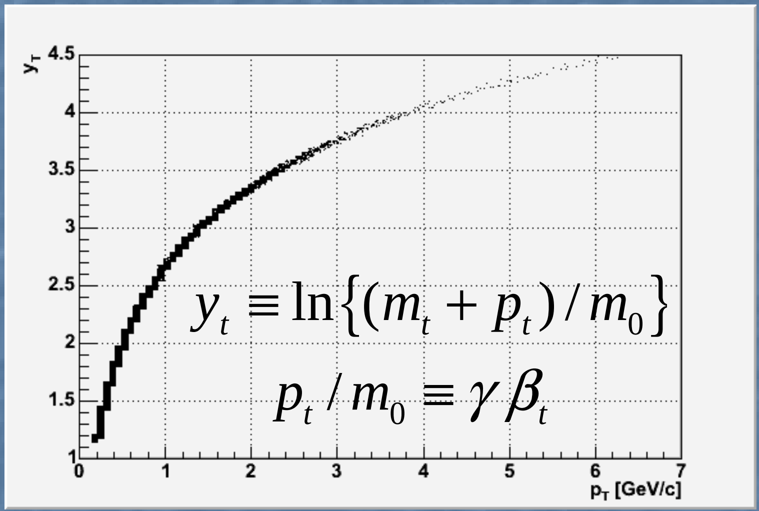

p_T=0.3 GeV → y_T=1.5

p_T=0.5 GeV → y_T=2.0

p_T=1 GeV → y_T=2.7

p_T=1.5 GeV → y_T= 3.1

- **Correlations will be plotted in p_T and y_T (which serves to emphasize the low p_T region).**
- **Shown are results for 200 GeV Au+Au, 62 GeV Au+Au, 200 GeV p+p, and 200 GeV d+Au collisions. y_T-y_T correlations are integrated over azimuth.**

Like-sign Near-side ($\Delta\phi$<60°) Correlations in Transverse Rapidity

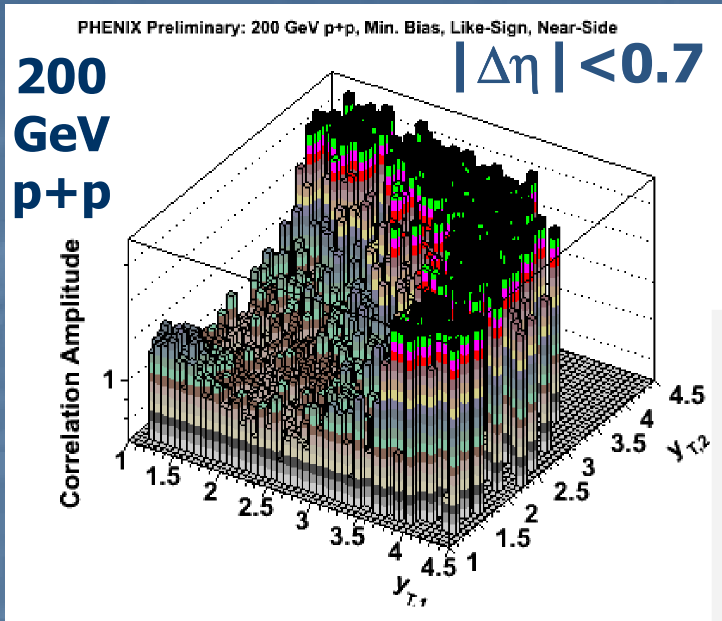

p_T=0.3 GeV → y_T=1.5

p_T=0.5 GeV → y_T=2.0

p_T=1 GeV → y_T=2.7

p_T=1.5 GeV → y_T= 3.1

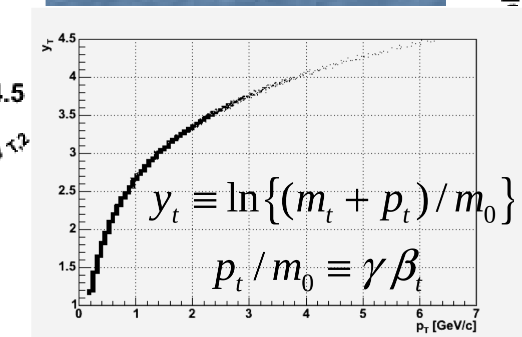

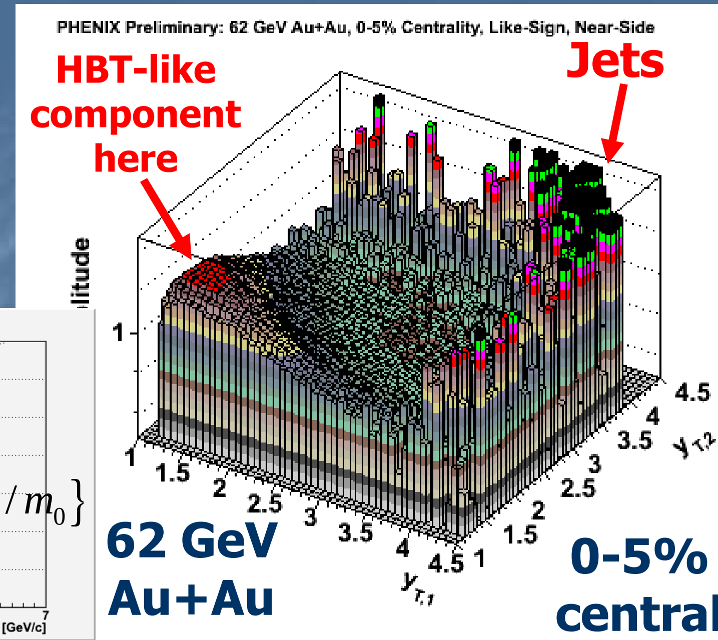

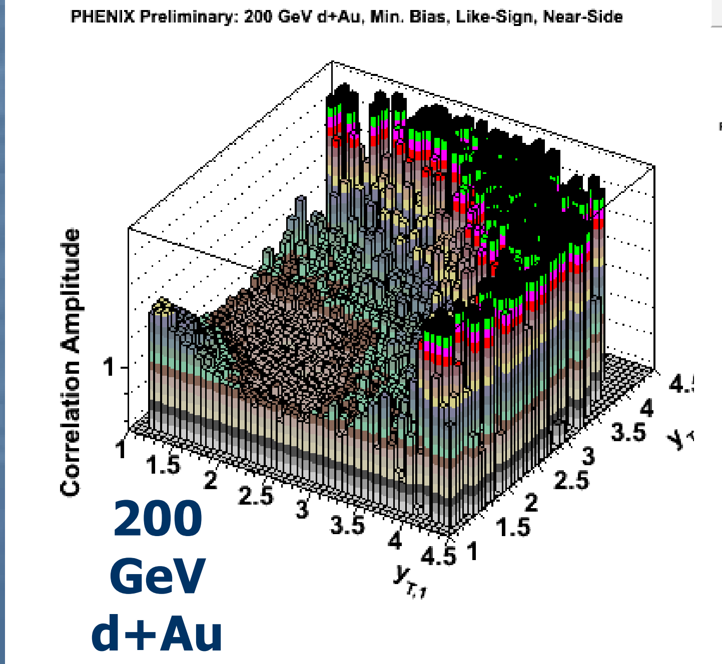

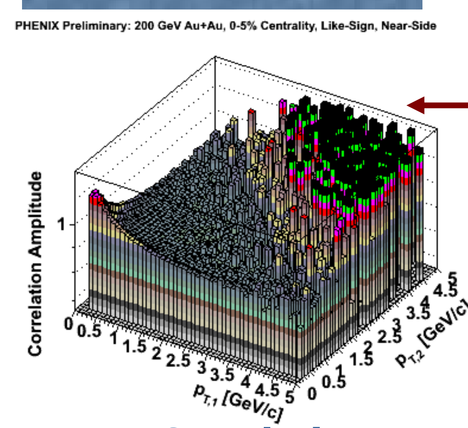

p_T-p_T Correlations

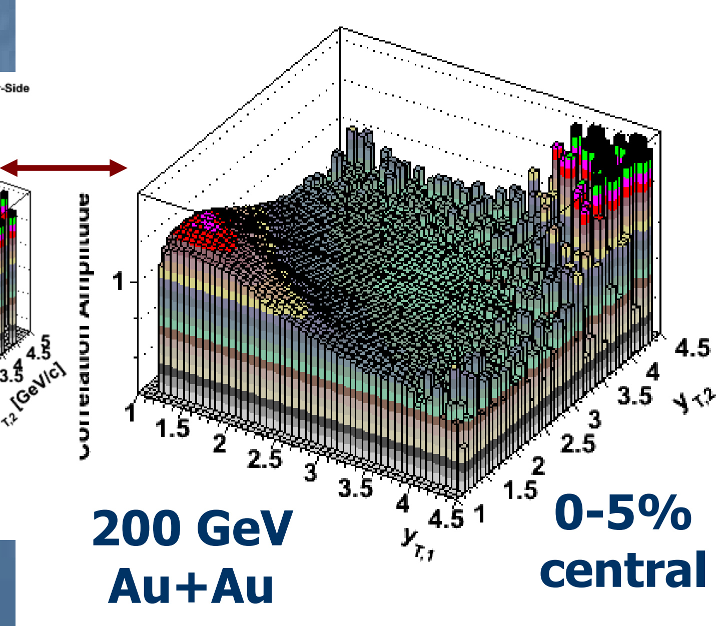

Like-sign Away-side ($\Delta\phi>120^o$) y_T Correlations

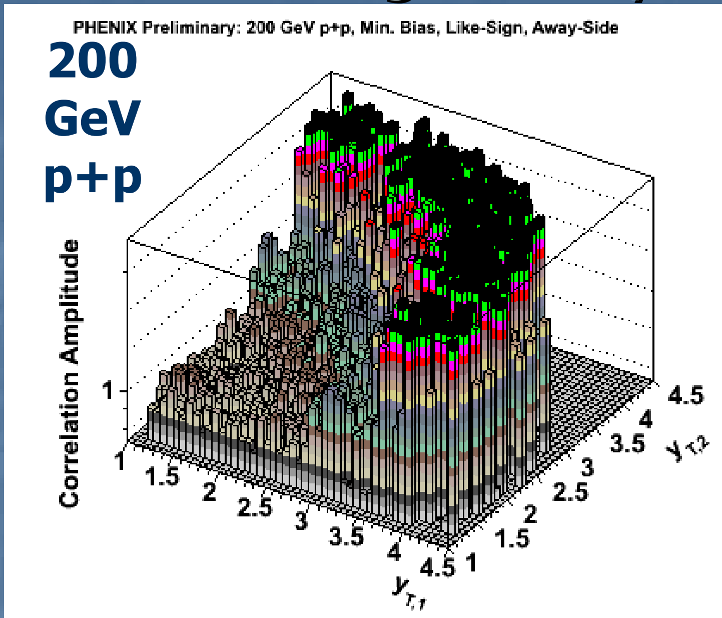

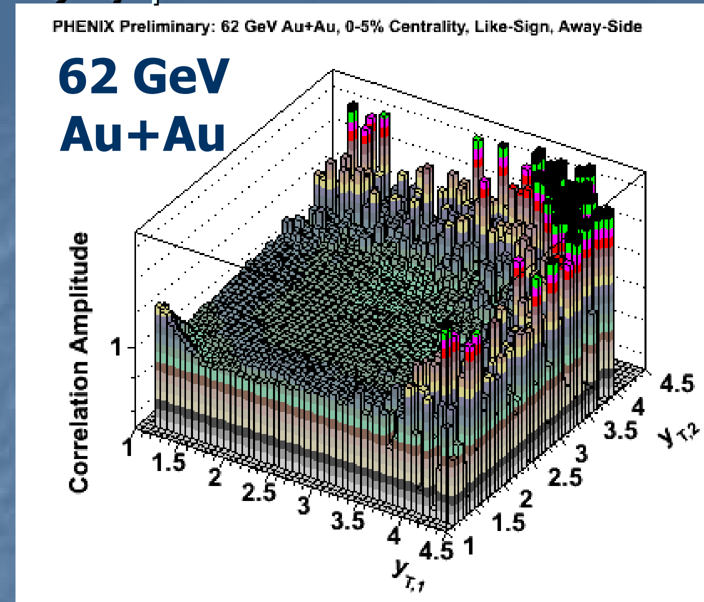

The jet structure persists, the peak with the HBT component does not. A low p_T correlation is observed in Au+Au collisions only for p_T<300 MeV/c. It's source is under investigation.

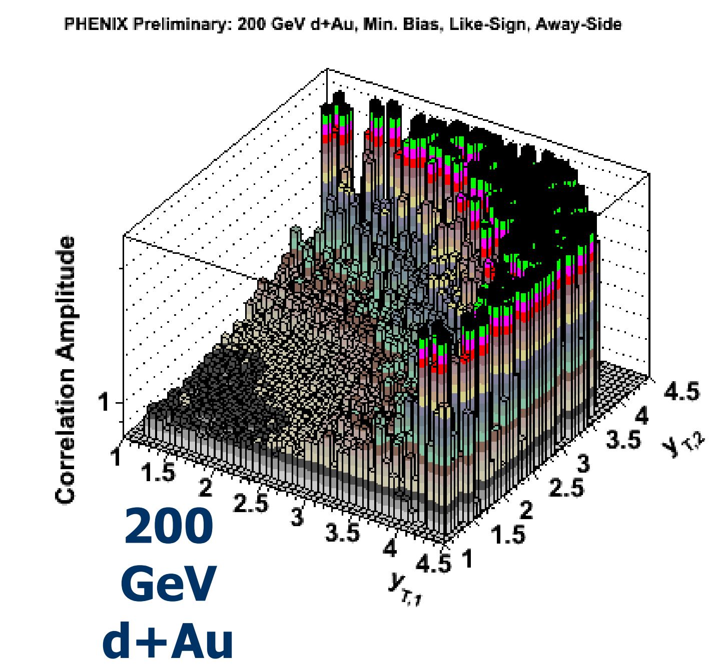

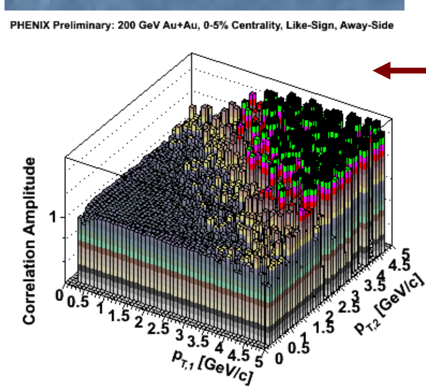

p_T-p_T Correlations

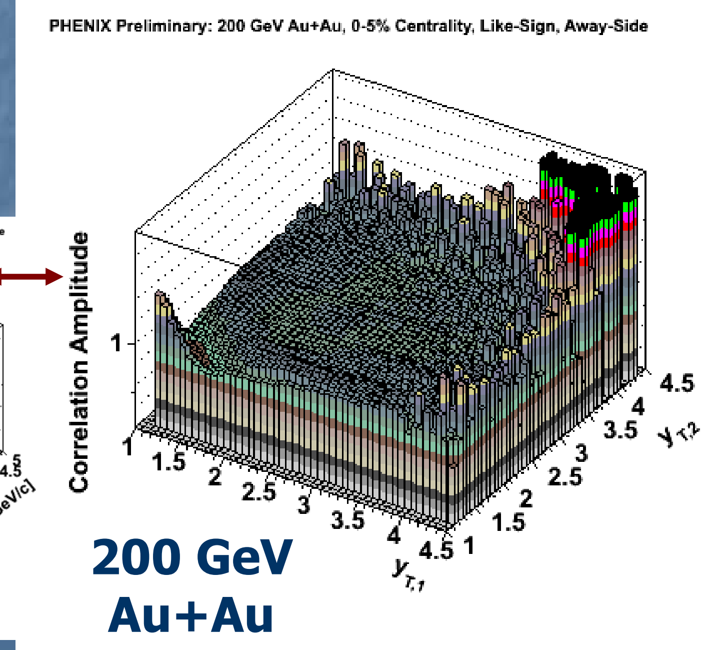

Unlike-sign Near-side ($\Delta\phi<60^o$) y_T Correlations

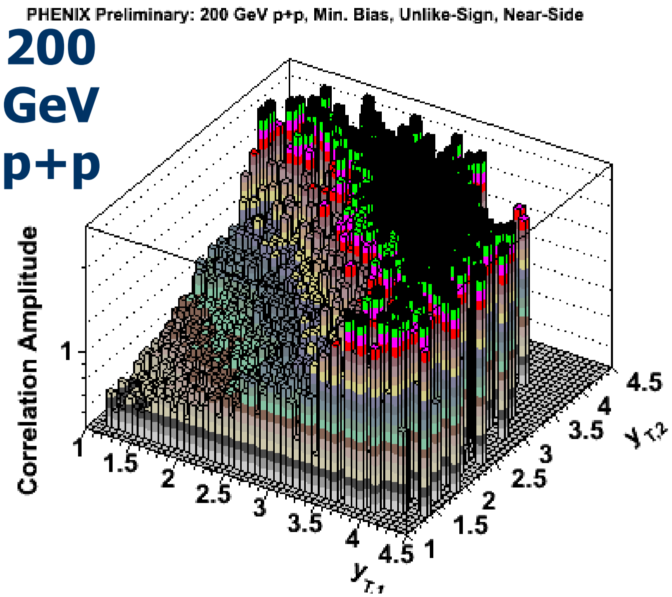

The jet structure persists, the broad peak with the HBT component on the near side does not.

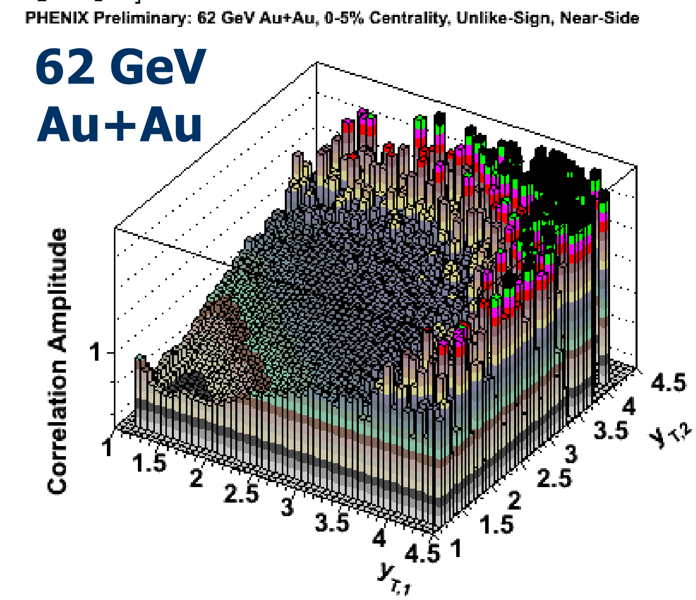

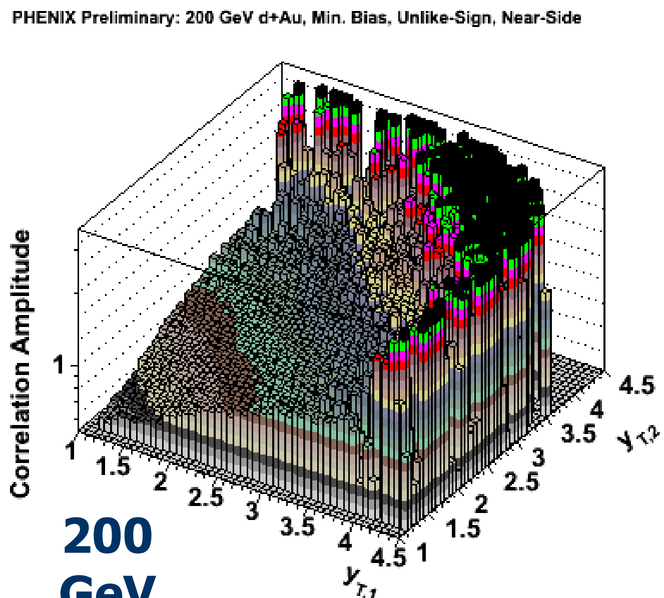

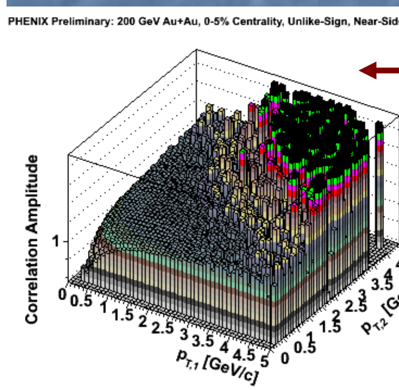

p_T-p_T Correlations

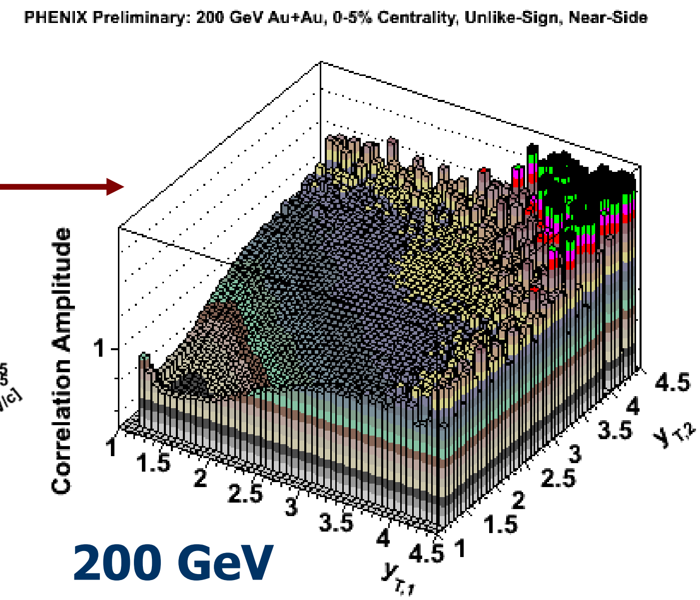

Unlike-sign Away-side ($\Delta\phi>120^{o}$) y_T Correlations

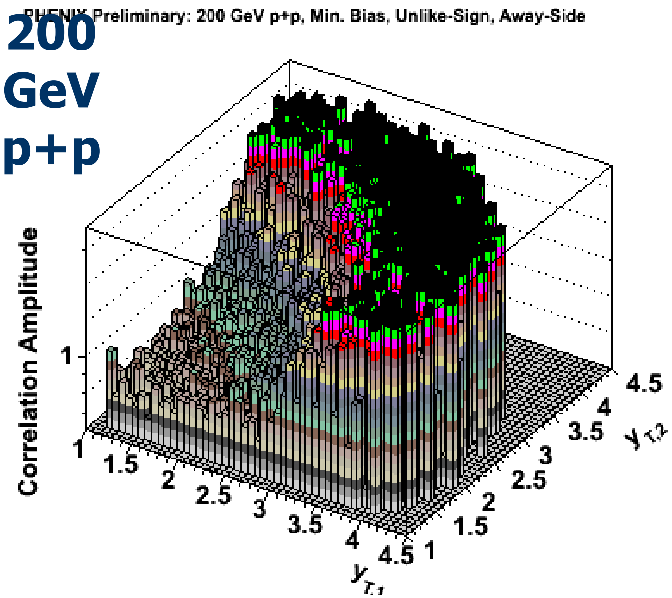

200 GeV p+p

The jet structure persists, the broad peak with the HBT component from like-sign near-side pairs does not.

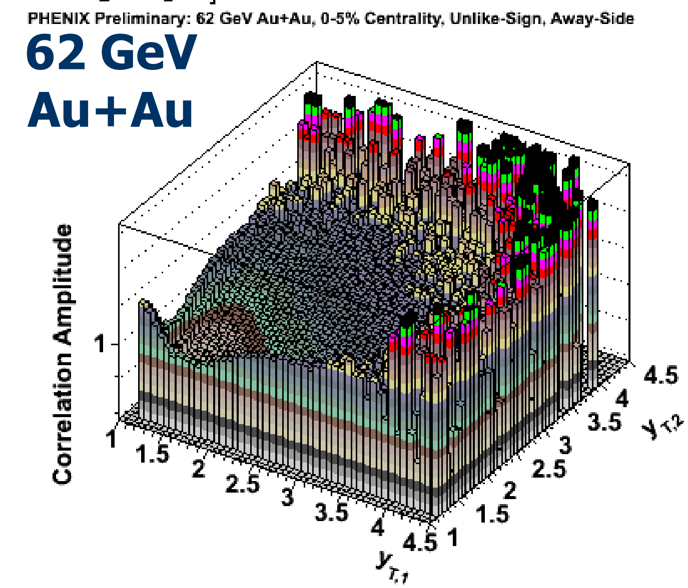

62 GeV Au+Au

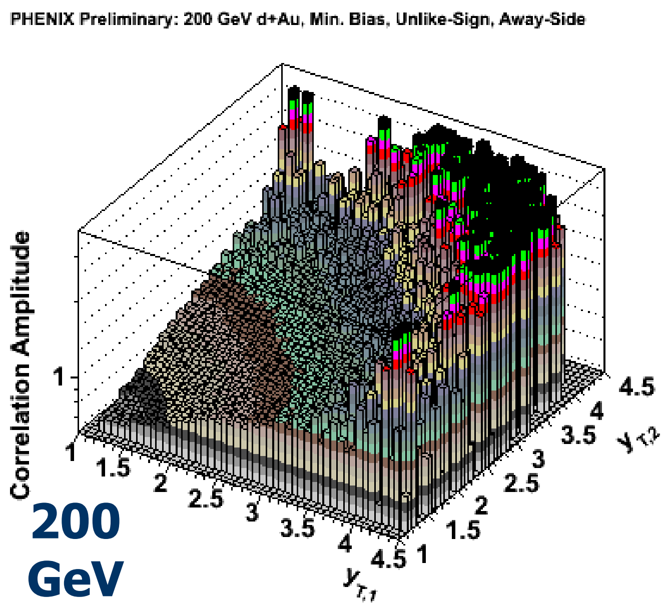

200 GeV d+Au

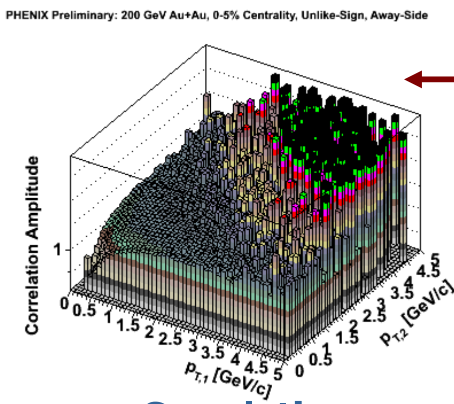

p_T-p_T Correlations

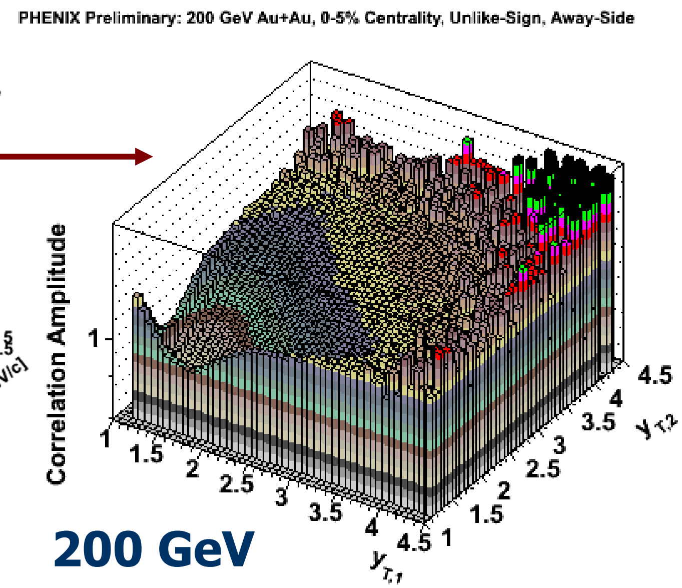

200 GeV Au+Au

Correlations Comparisons along a $y_{T,1}=y_{T,2}$ bin slice

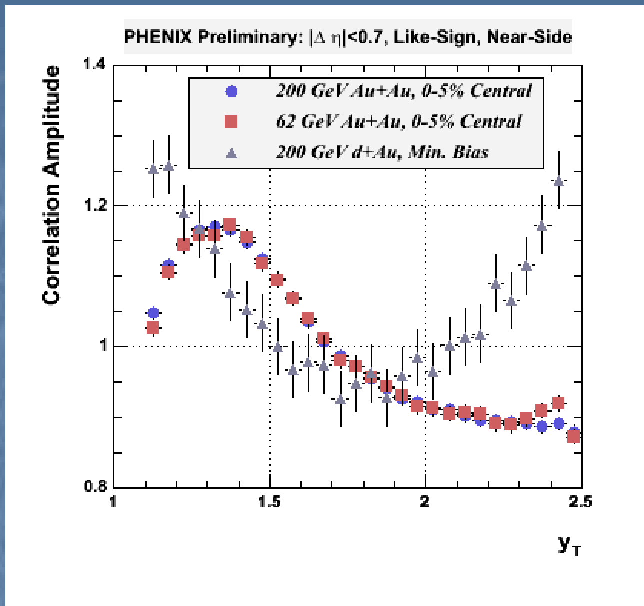

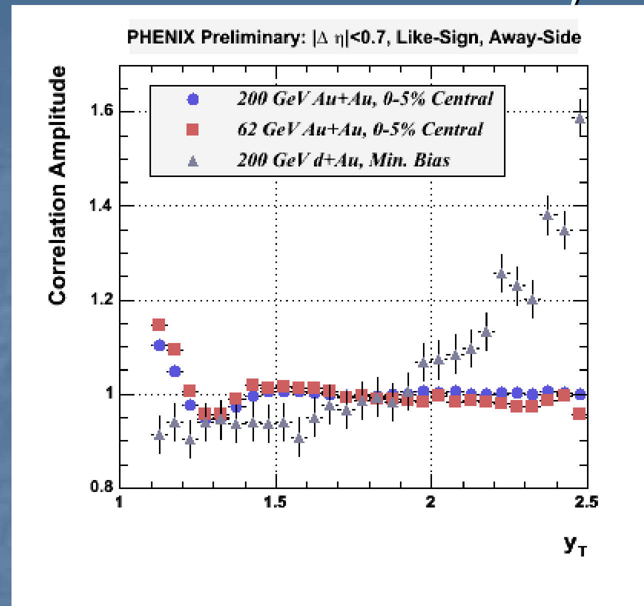

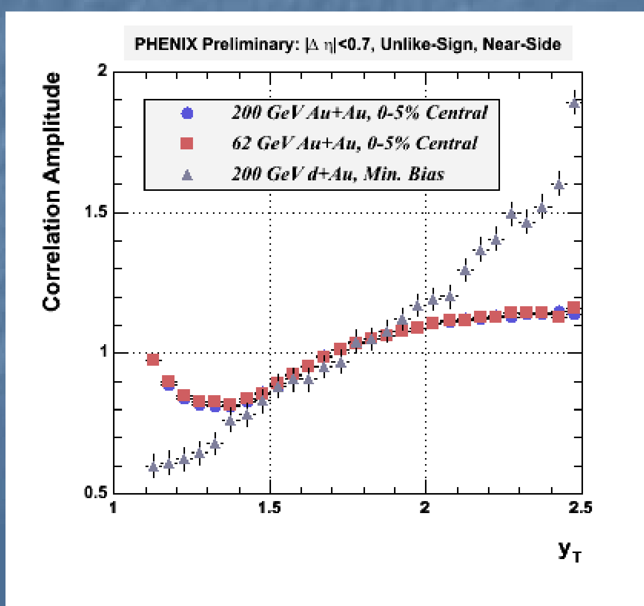

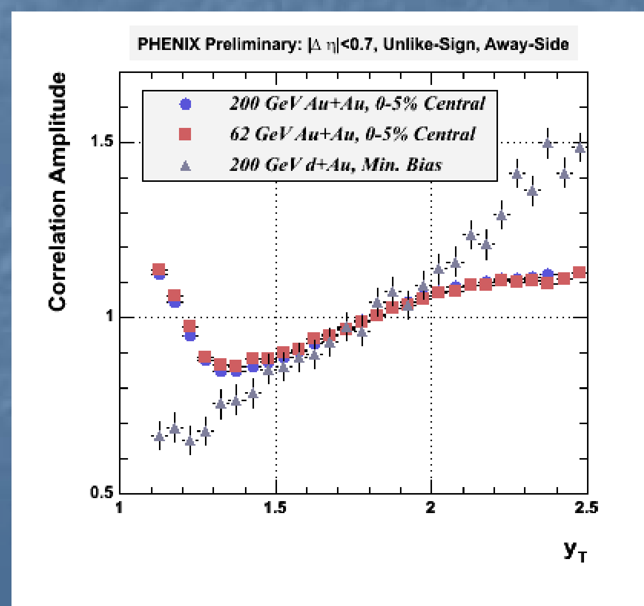

p_T=0.25 GeV → y_T=1.34

p_T=0.3 GeV → y_T=1.5

p_T=0.5 GeV → y_T=2.0

p_T=0.9 GeV → y_T=2.56

p_T=1.5 GeV → y_T= 3.1

- **The 62 GeV and 200 GeV Au+Au distributions are similar.**
- **The behavior at low p_T between Au+Au and d+Au collisions is different in all 4 cases.**
- **The influence of resonance and conversion contributions is under investigation.**

Like-sign Near-side ($\Delta\phi<60^o$) y_T Correlations

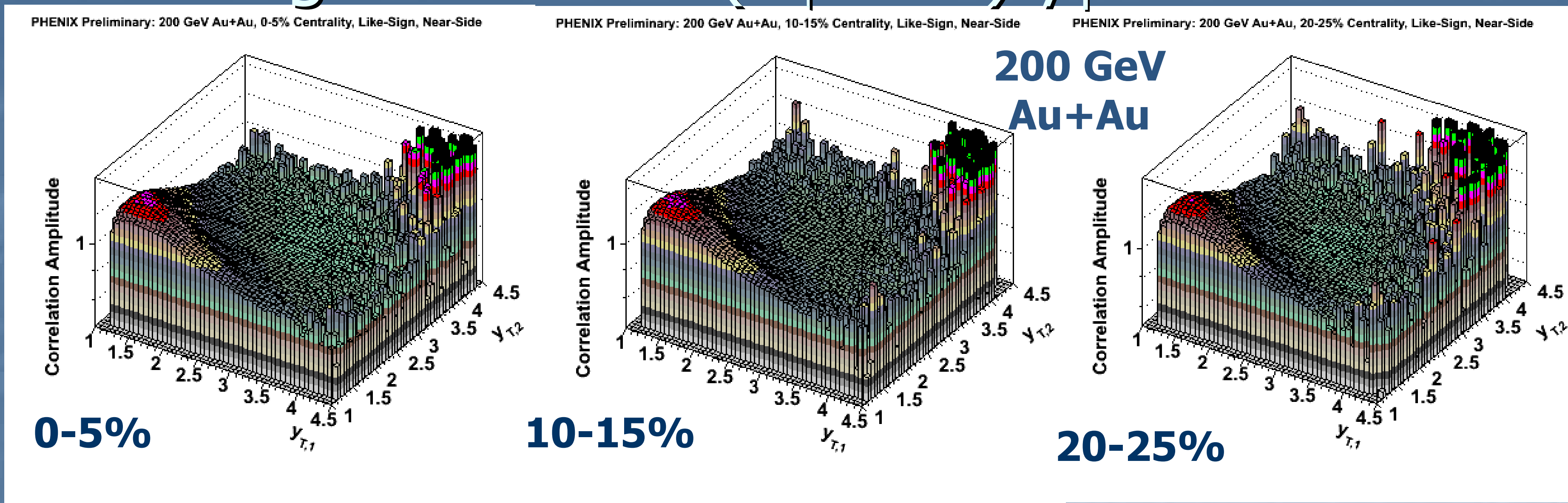

The primary features persist from central to peripheral collisions. Correlations for the most peripheral collisions are similar to d+Au collisions. This statement is true for all 4 cases.

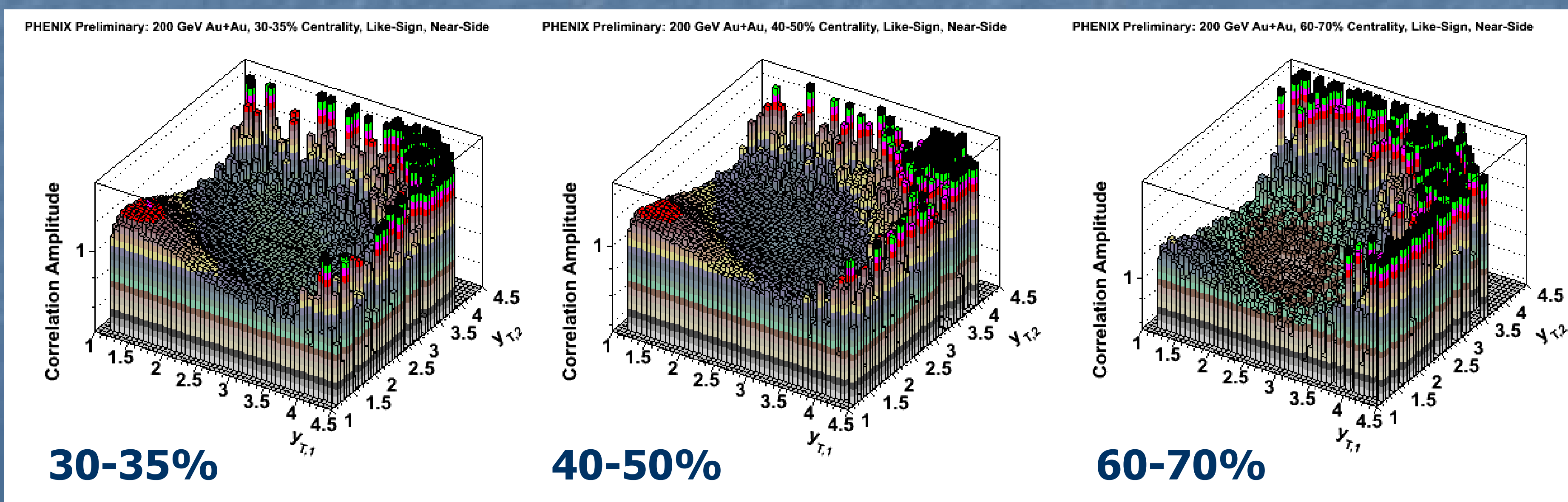

Correlations Comparisons along a $y_{T,1}=y_{T,2}$ bin slice

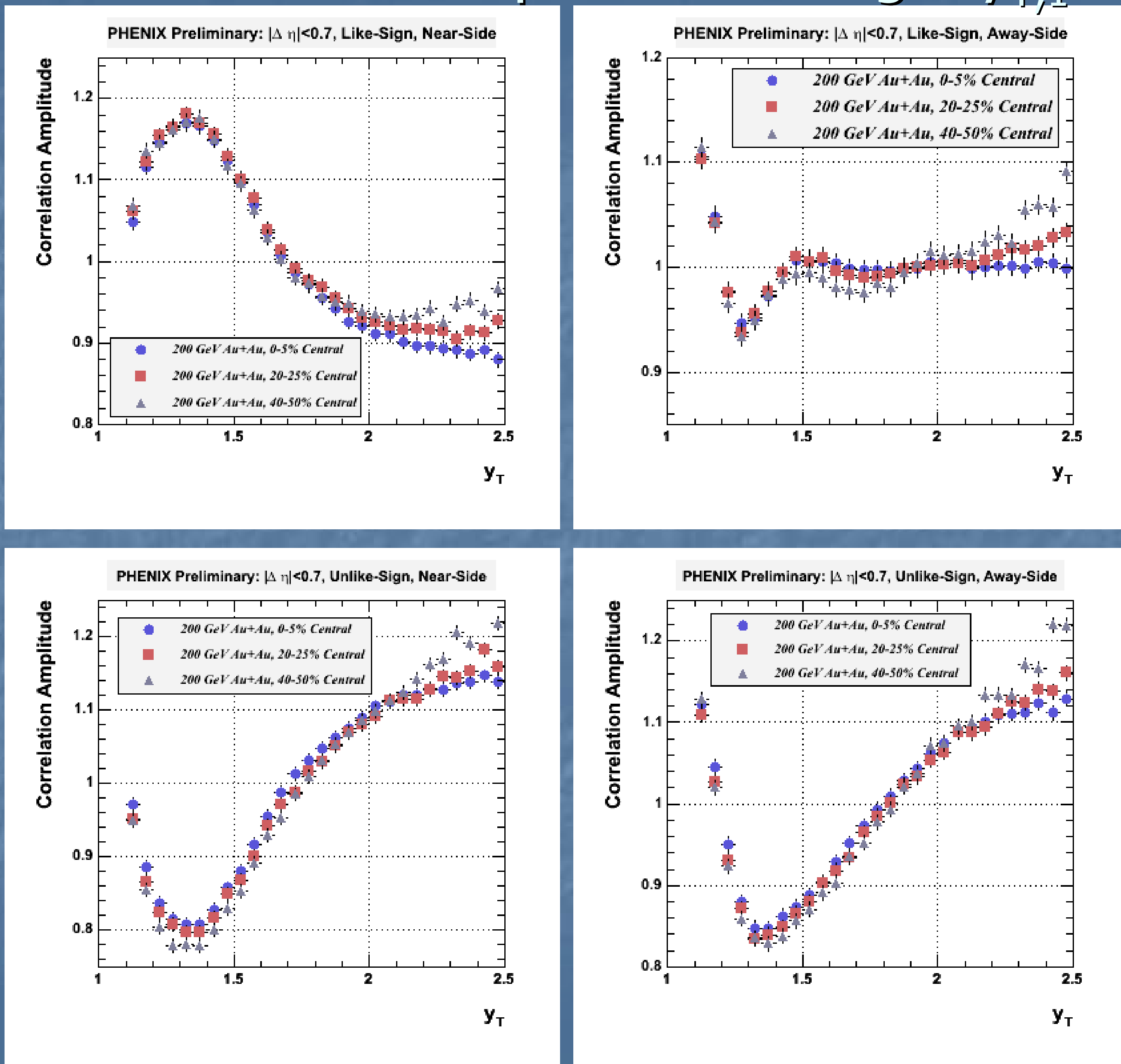

p_T=0.25 GeV → y_T=1.34

p_T=0.3 GeV → y_T=1.5

p_T=0.5 GeV → y_T=2.0

p_T=0.9 GeV → y_T=2.56

p_T=1.5 GeV → y_T= 3.1

The integrated correlation amplitudes vary little over a wide range of centralities (and pair occupancies). Later, background and flow-subtracted peak amplitudes will be measured.

Charge Difference Correlations: C(LS)-C(US): Near Side

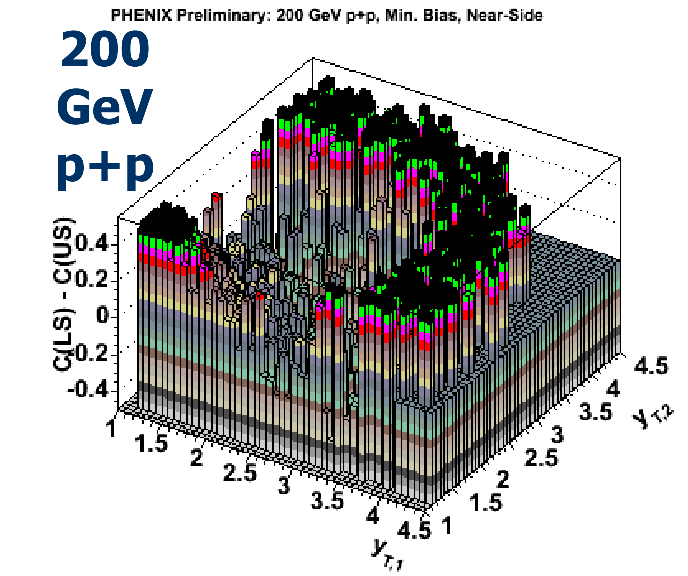

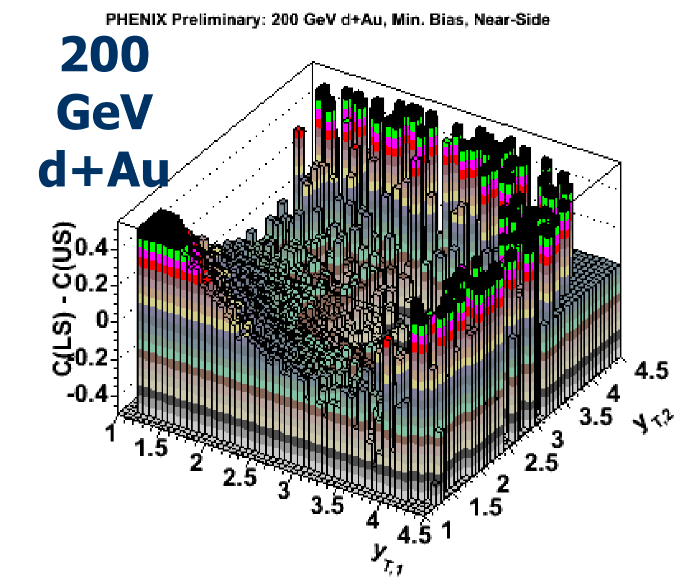

Calculated by subtracting the correlation amplitude of unlike-sign pairs from that of like-sign pairs. It is expected that primarily HBT remains in this case at low y_T. The remaining peak is much broader in Au+Au collisions and shifted in y_T compared to p+p and d+Au collisions. The location of the peaks in y_T agree with STAR results.

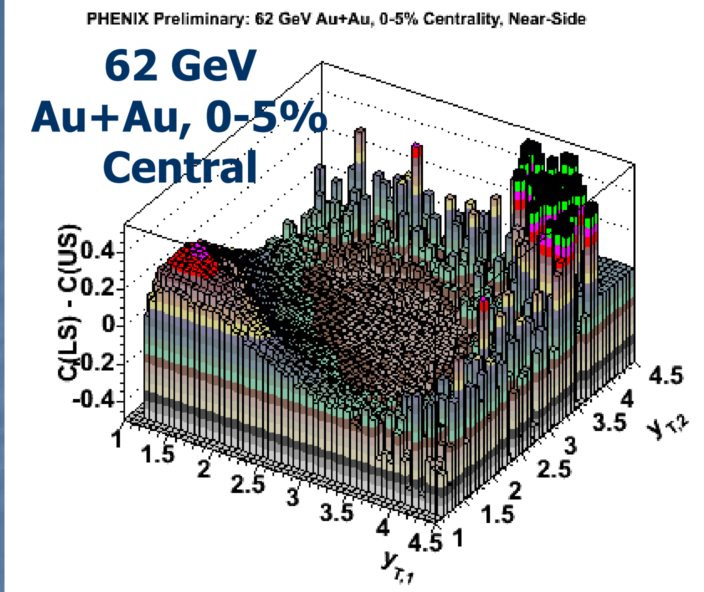

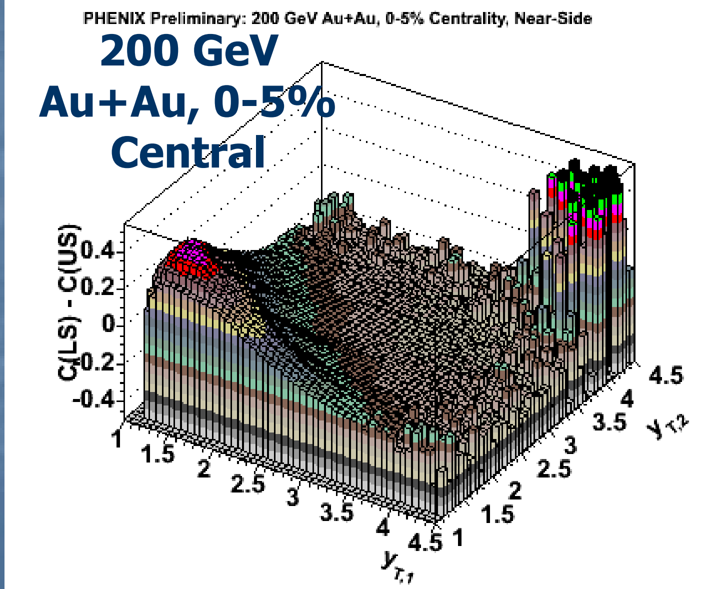

Charge Difference Correlations: C(LS)-C(US): Away Side

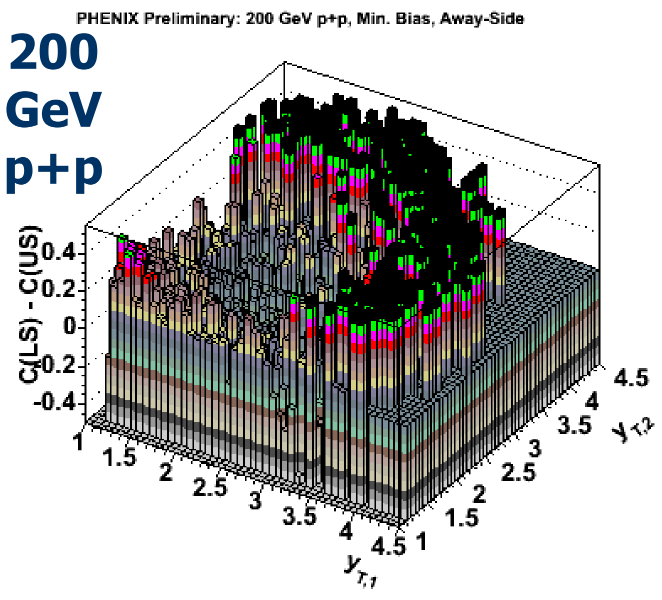

200 GeV p+p

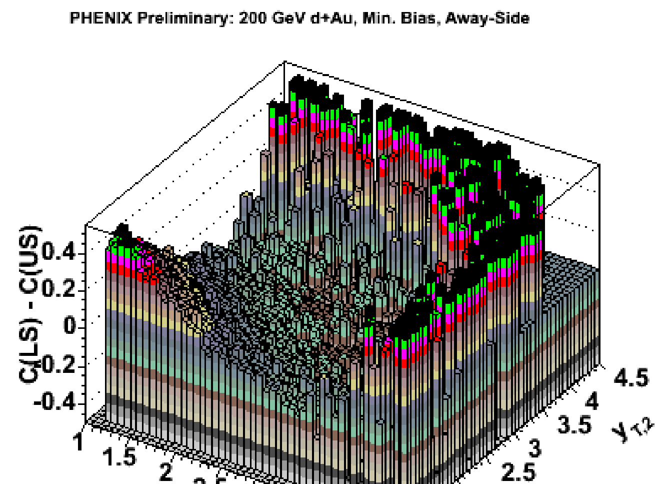

200 GeV d+Au

A similar peak with similar properties compared to the near-side is seen on the away-side, but with a lower integrated correlation amplitude.

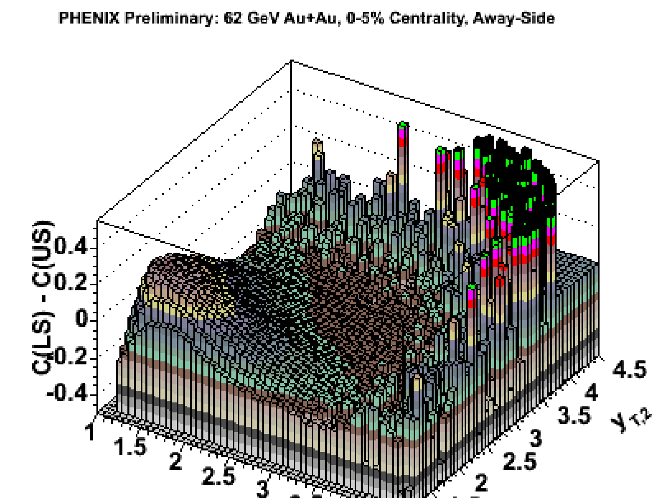

62 GeV Au+Au, 0-5% Central

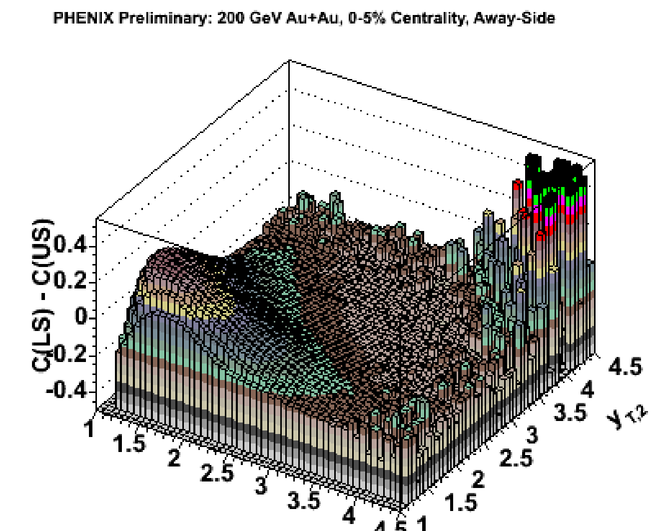

200 GeV Au+Au, 0-5% Central

Charge Difference Correlations Comparisons along a $y_{T,1}=y_{T,2}$ bin slice

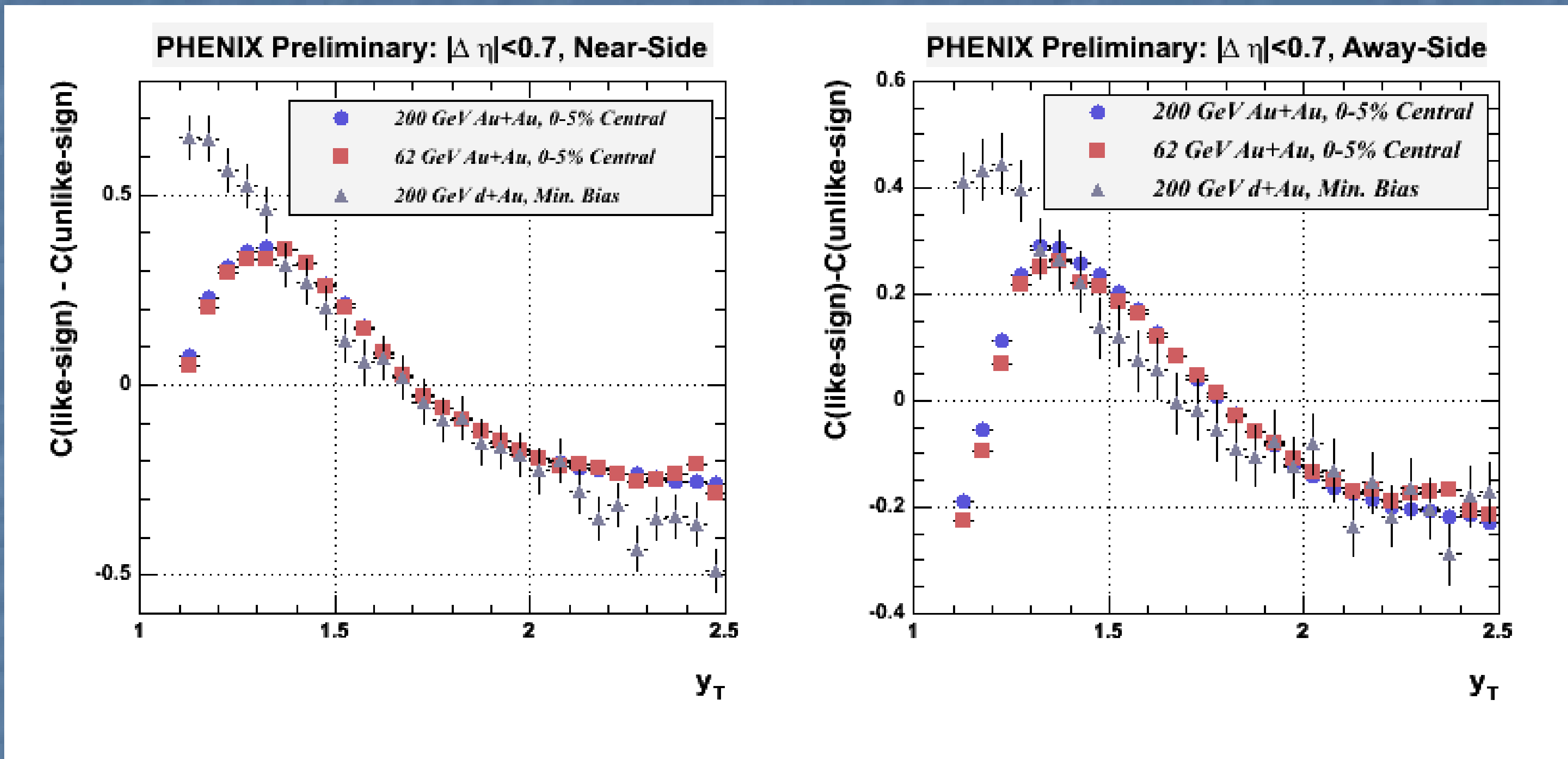

The near and away side charge difference correlations are qualitatively similar. The p+p and d+Au charge difference correlations do not decrease significantly at low y_T.

Near-Side Peak Amplitude vs. Centrality

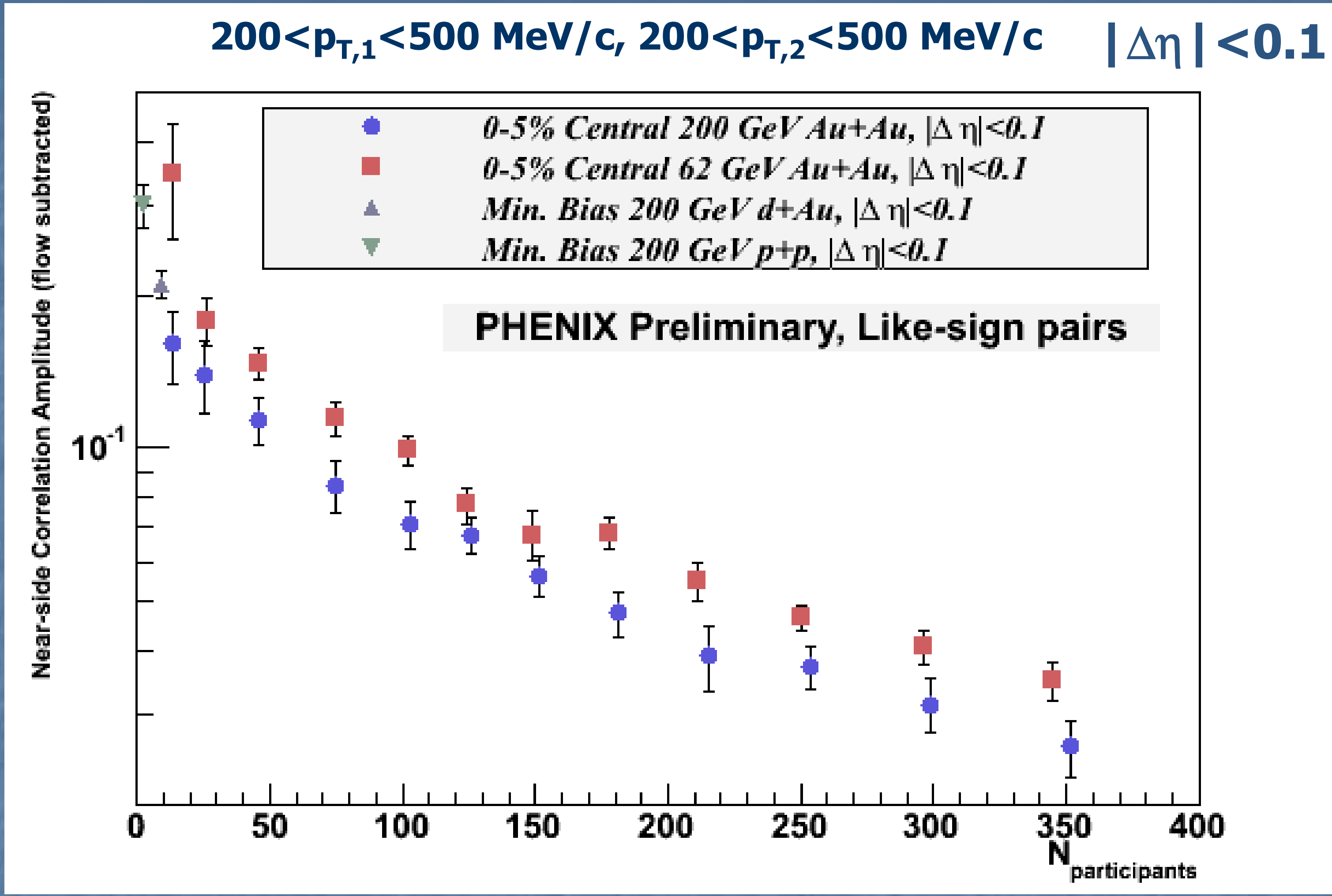

Azimuthal correlation functions were measured for all like-sign pairs with both pairs in the p_T range from 200-500 MeV (y_T<2). The near-side peak was fit to a Gaussian convoluted with a Background*cos(2Δϕ) flow term (Au+Au only). For |Δη|<0.1, the like-sign pairs are correlated in $Q_{invariant}$ space, the unlike-sign pairs are not.

Near-Side Peak Amplitude vs. Centrality

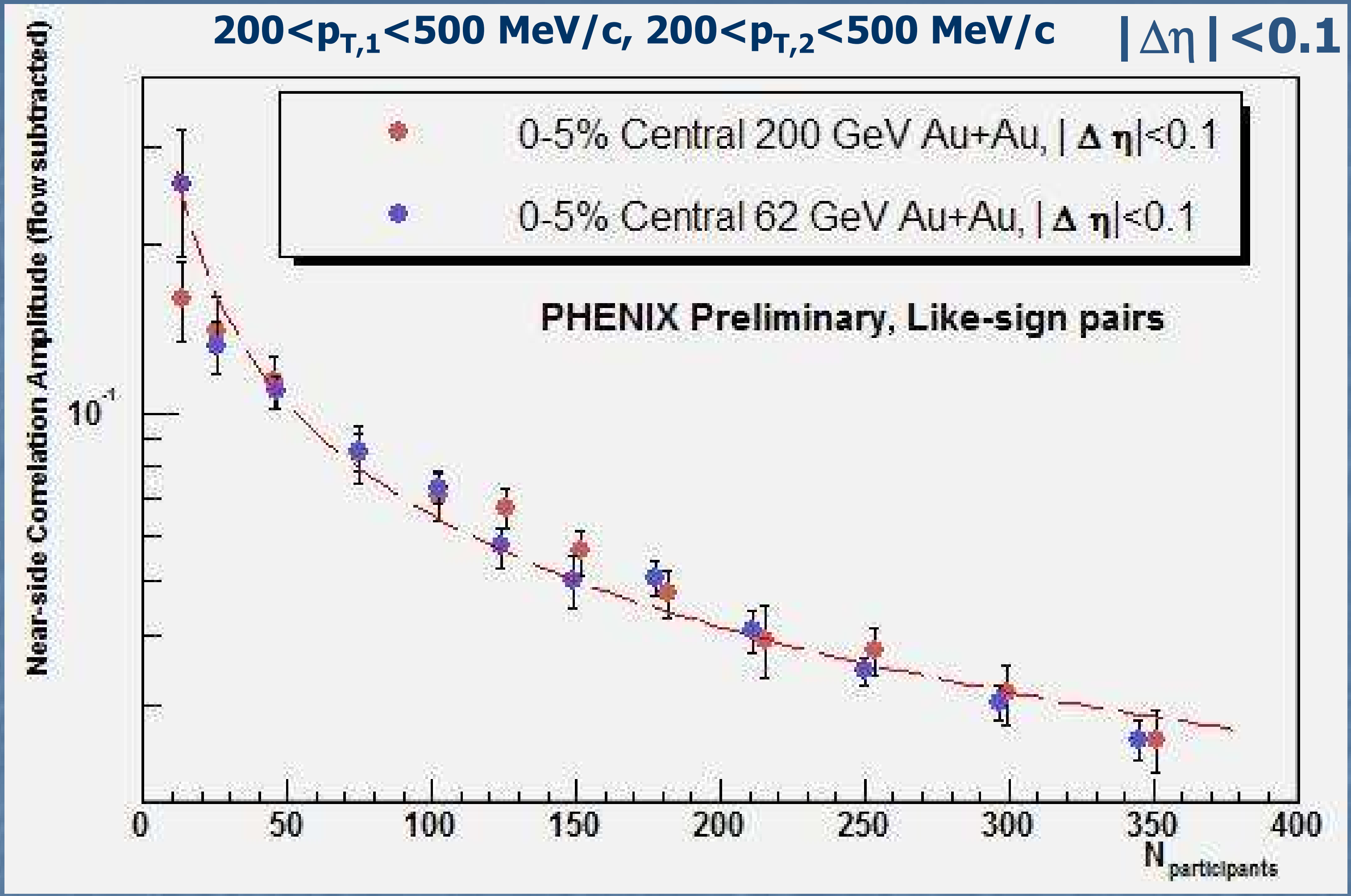

The universal curves can be described by a power law function of N_{part}.

Near-Side Peak Amplitude vs. p_T

$p_{T,min}<p_{T,1}<p_{T,max}$, $p_{T,min}<p_{T,2}<p_{T,max}$

Points plotted in the center of each p_T bin.

$|\Delta\eta|<0.1$

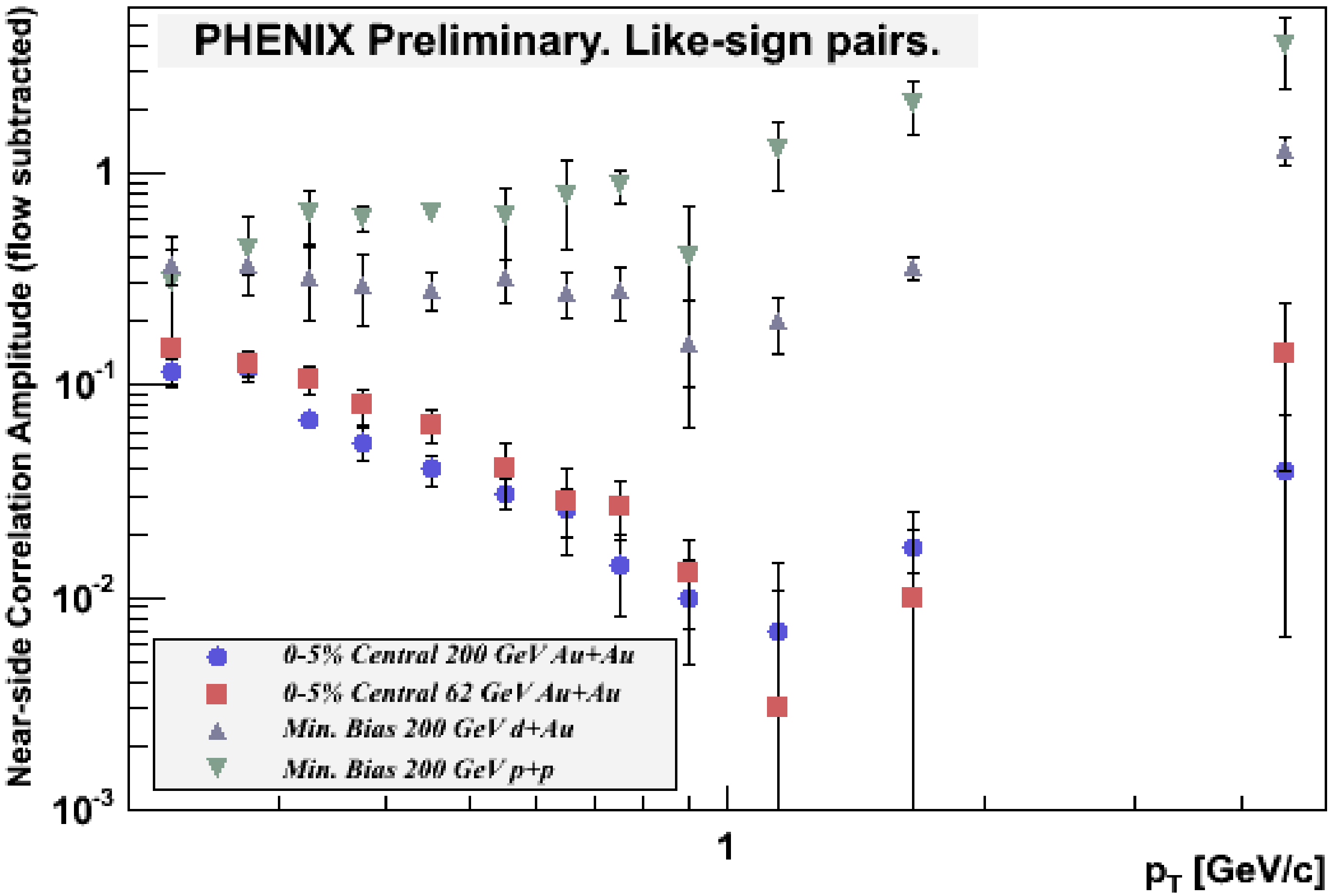

p_T bin widths have been chosen such that the mean number of pairs per event is the same in each bin.

Central Au+Au flow- and background-subtracted amplitudes decrease exponentially with p_T while the p+p and d+Au amplitudes remain flat. The amplitude increase above 1 GeV is due to the contribution of hard processes. No evidence for excess contributions from hard processes is seen in Au+Au collisions in the p_T=0.5-1.0 GeV/c range.

Just for Fun: A Critical Exponent Analysis

- Let's assume that the increased fluctuations are indicative of critical behavior. Then, it is expected that a) the system can be described by critical exponents, and b) all systems can be described by the same set of critical exponents. Recall that

$$\frac{\left(\sigma^2/\mu\right)}{\mu} = \frac{1}{k_{NBD}} + \frac{1}{\mu} = \frac{k_B T}{V} k_T$$

- The critical exponent for compressibility is represented by the symbol γ and is described by $\frac{k_T}{k_T^c} = A'\left(\frac{T-T_c}{T_C}\right)^{-\gamma}$
- Replacing and solving for $1/k_{NBD}$ gives (A=constant, T=Temperature, V=volume)

$$\frac{1}{k_{NBD}} + \frac{1}{\mu} = \frac{\left(\sigma^2/\mu\right)}{\mu} = A\left(\frac{T}{V}\right)\left(\frac{T-T_c}{T_C}\right)^{-\gamma}$$

N.B.D. 1/k+1/μ

All systems have been scaled to match the 200 GeV Au+Au points for emphasis.

All four systems exhibit a power law behavior with respect to N_{part}. All systems appear to follow a universal curve within errors.

The fit assumes that $N_{part,c}$~0

$$T \propto N_{part}^{p}$$

The value of the critical exponent is γ=1.24±0.13 (p=1/3), γ=1.1±0.1 (p→0), for all species.

This is consistent with γ for common gas-liquid phase transitions, which are typically between 1.2 and 1.3.

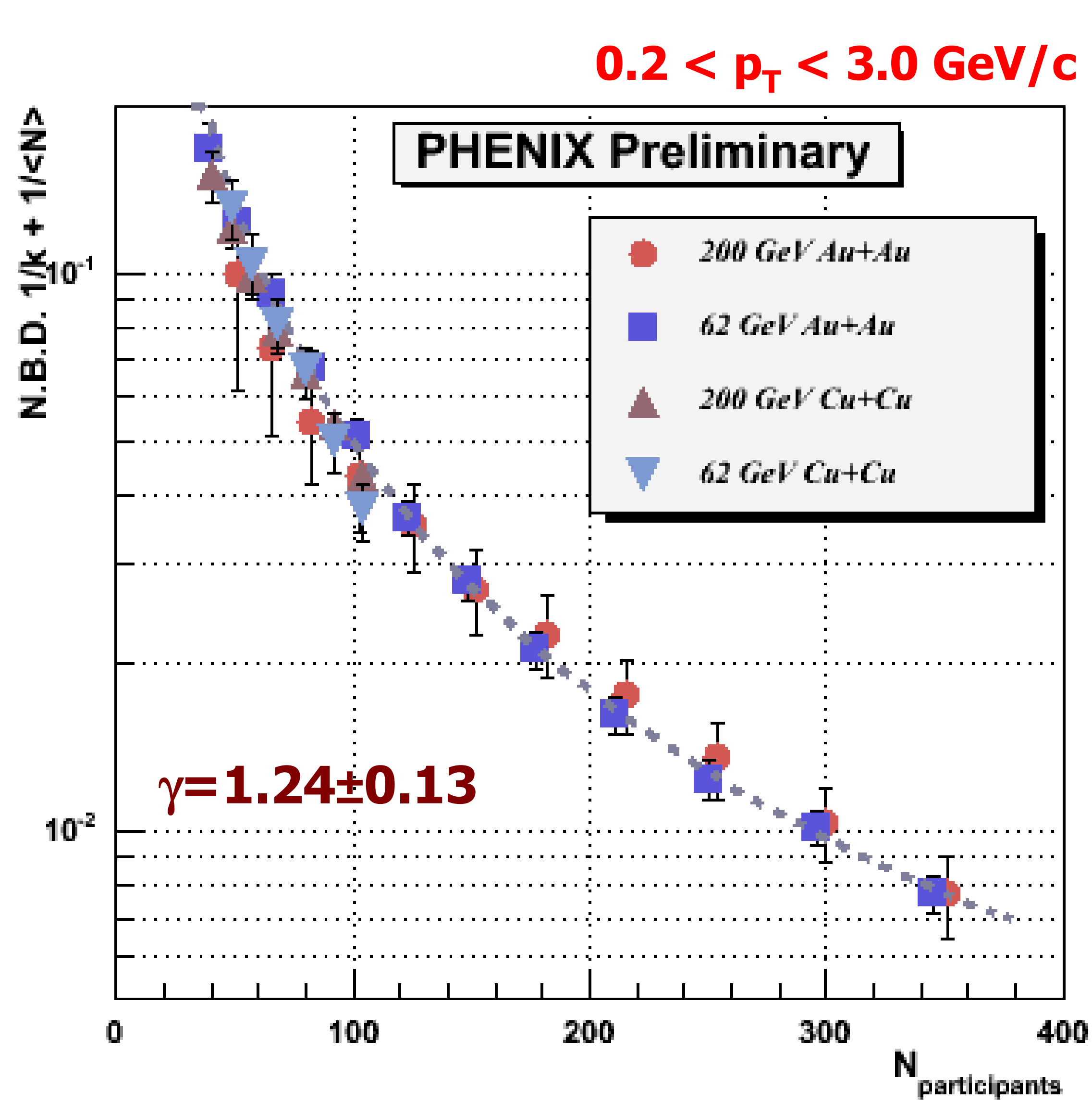

Critical Exponents vs. $N_{part,c}$

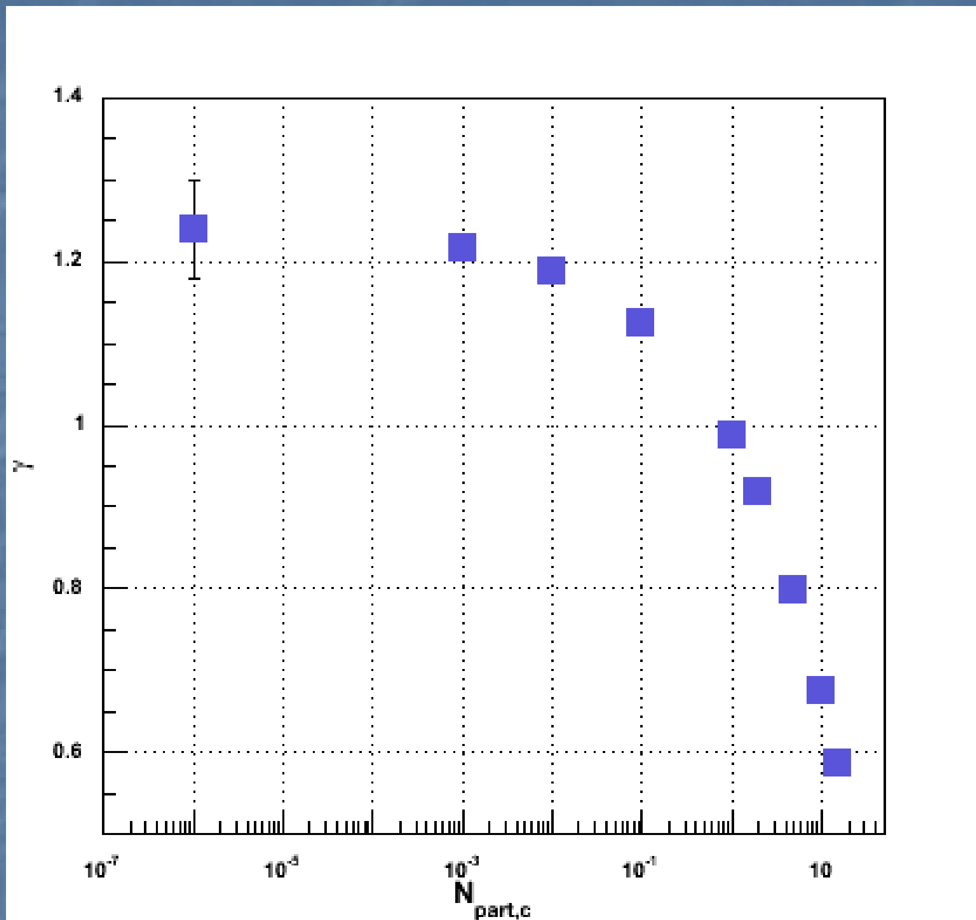

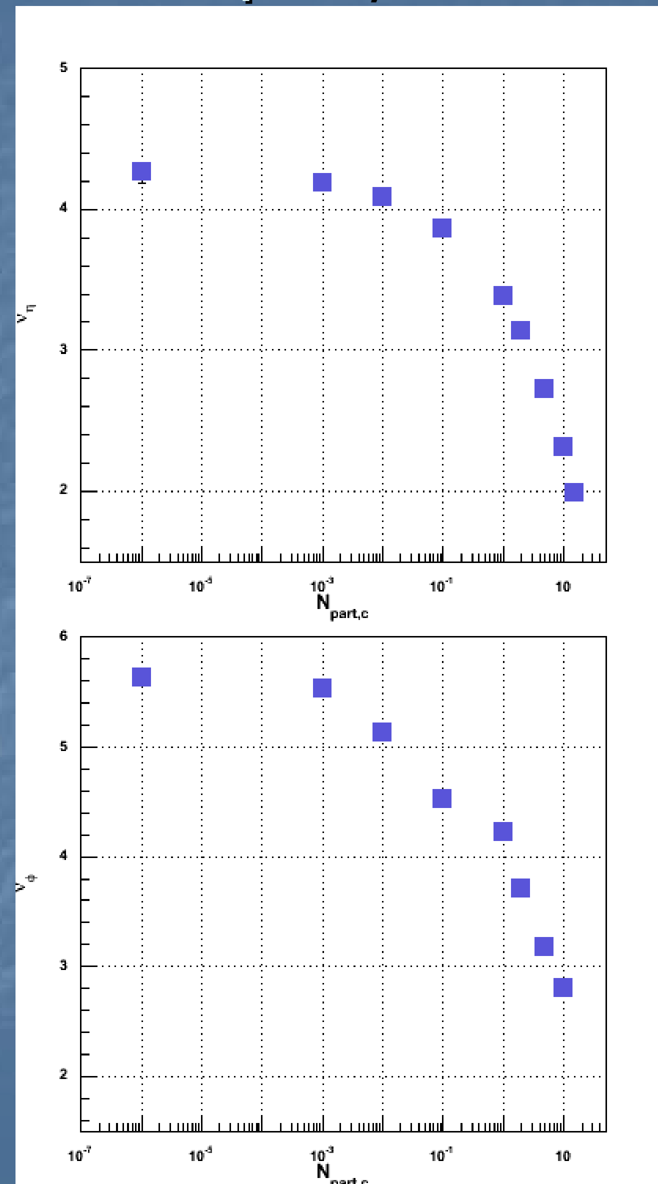

The critical exponents from the fits are sensitive to $N_{part,c}$ above about 0.1

Conclusions

- PHENIX has presented a survey of multiplicity fluctuations as a function of collision species, collision energy, centrality, and p_T range.
  - The fluctuations increase with a power law behavior as centrality decreases.
  - All species measured can be described by a universal power law curve.
- PHENIX has presented a survey of correlation length measurements using multiplicity fluctuations
  - Correlation lengths at low p_T exhibit a maximum at N_{part}=100.
  - Correlation lengths are smaller than similar measurements at the AGS.
  - Correlation lengths increase with decreasing beam energy.
  - Correlation lengths increase at low p_T.
  - Correlation lengths as a function of N_{part} (N_{part}>100) for all species can be described by a universal power law curve.
- PHENIX has presented a survey of two-particle p_T correlations at low p_T in Au+Au, d+Au, and p+p.
  - Significant differences in like-sign near-side correlations are seen between p+p and d+Au at low p_T.
  - Near-side correlation amplitudes in Au+Au as a function of p_T exhibit a distinct boundary between the contribution of "soft" correlations and "hard" correlations.

Auxiliary Slides

Acceptance and Occupancy Corrections: Results Extrapolated to 2π Acceptance

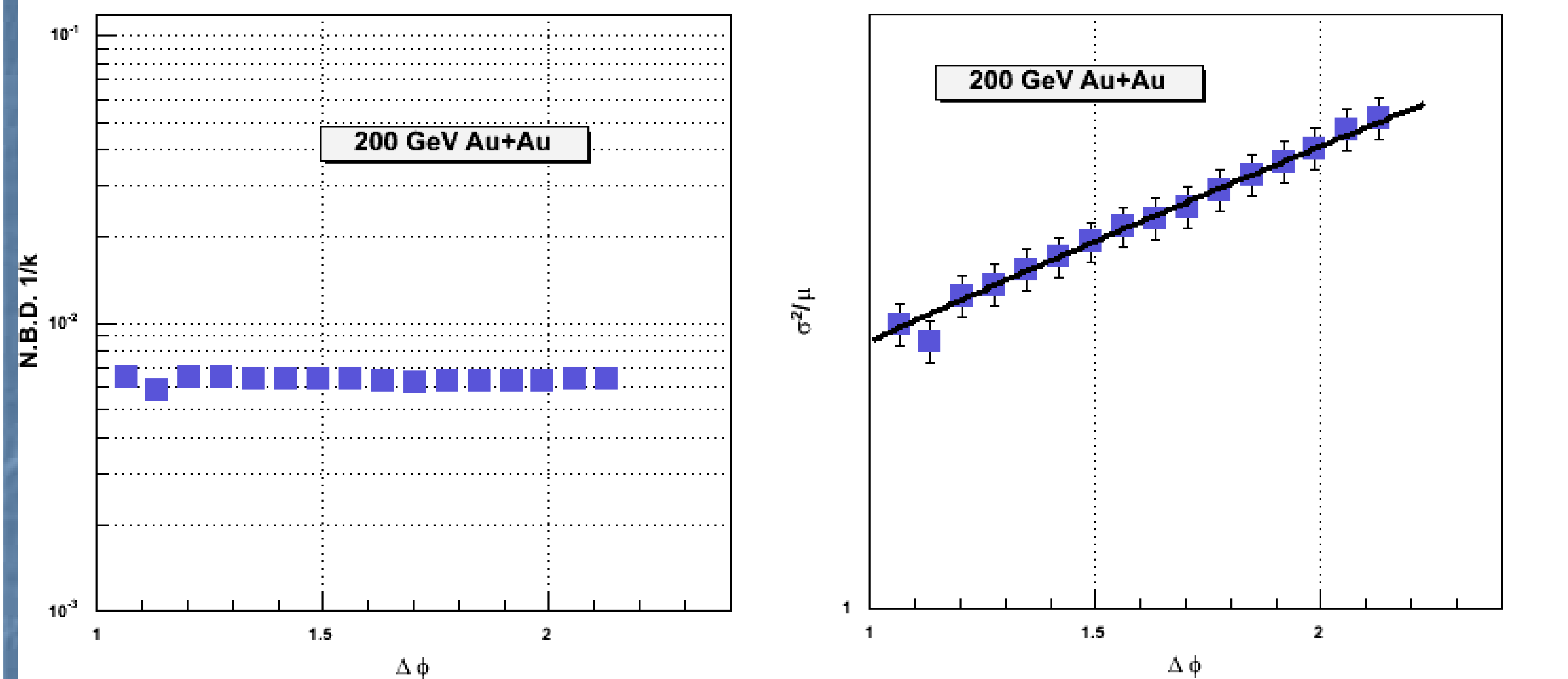

Multiplicity fluctuations are acceptance dependent. PHENIX results shown here are projected to 2p acceptance to facilitate direct comparisons to other measurements.

A Survey of N.B.D. 1/k

- Inclusive charged hadron fluctuations.
- These values are corrected to remove the contribution due to impact parameter (geometrical) fluctuations and projected to 2π in azimuth for direct comparisons to NA49.
- Here, the Poissonian (random) limit is $1/k \rightarrow 0$.
- Large non-random fluctuations are observed that decrease with centrality.

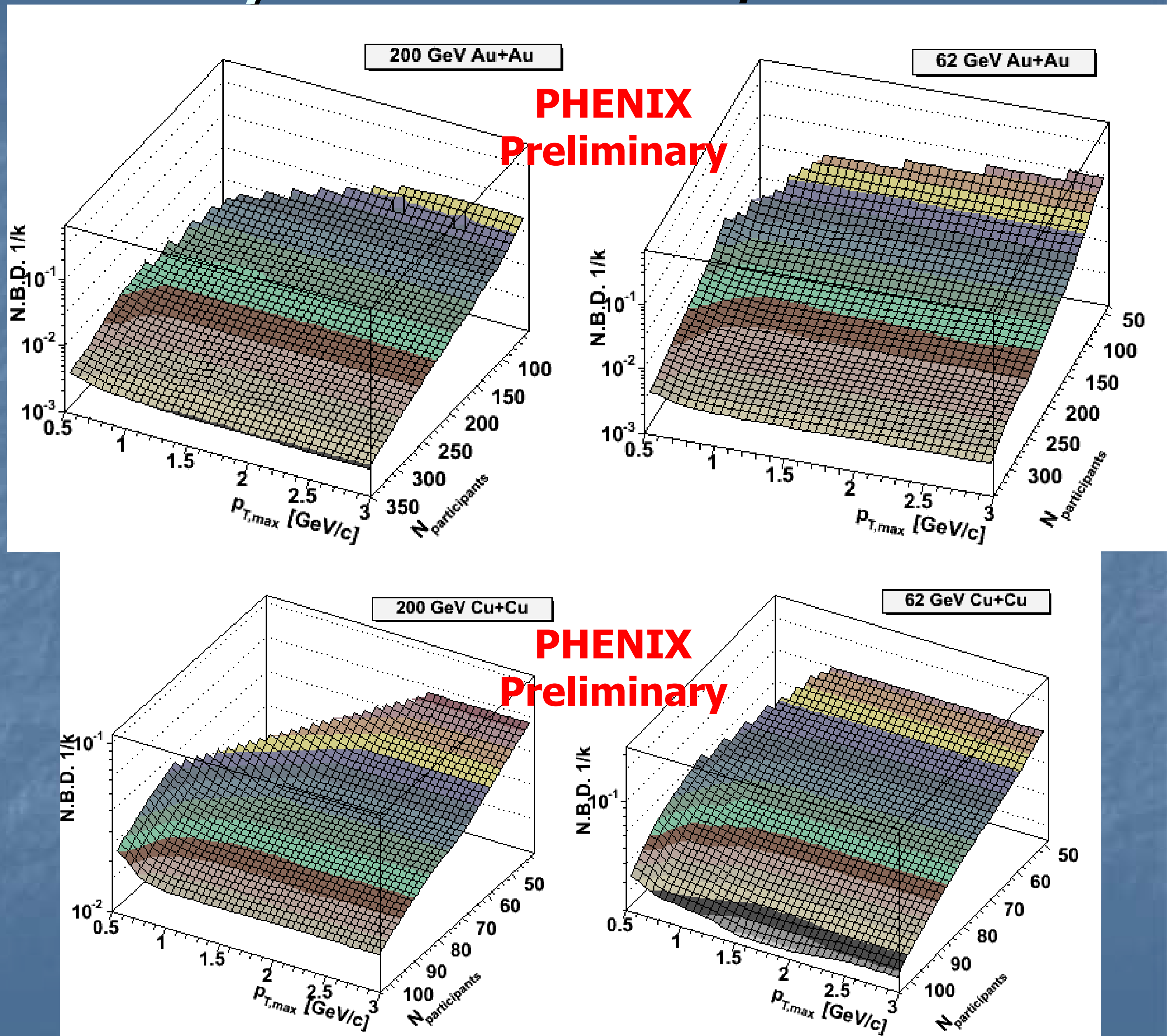

Jet Simulation Results: PHENIX at sqrt(s_{NN}) = 200 GeV

The S_{prob} parameter is initially adjusted so that F_{pT} from the simulation matches F_{pT} from the data for 20-25% centrality (circled). It is then FIXED and finally scaled by R_{AA} for all other centralities.

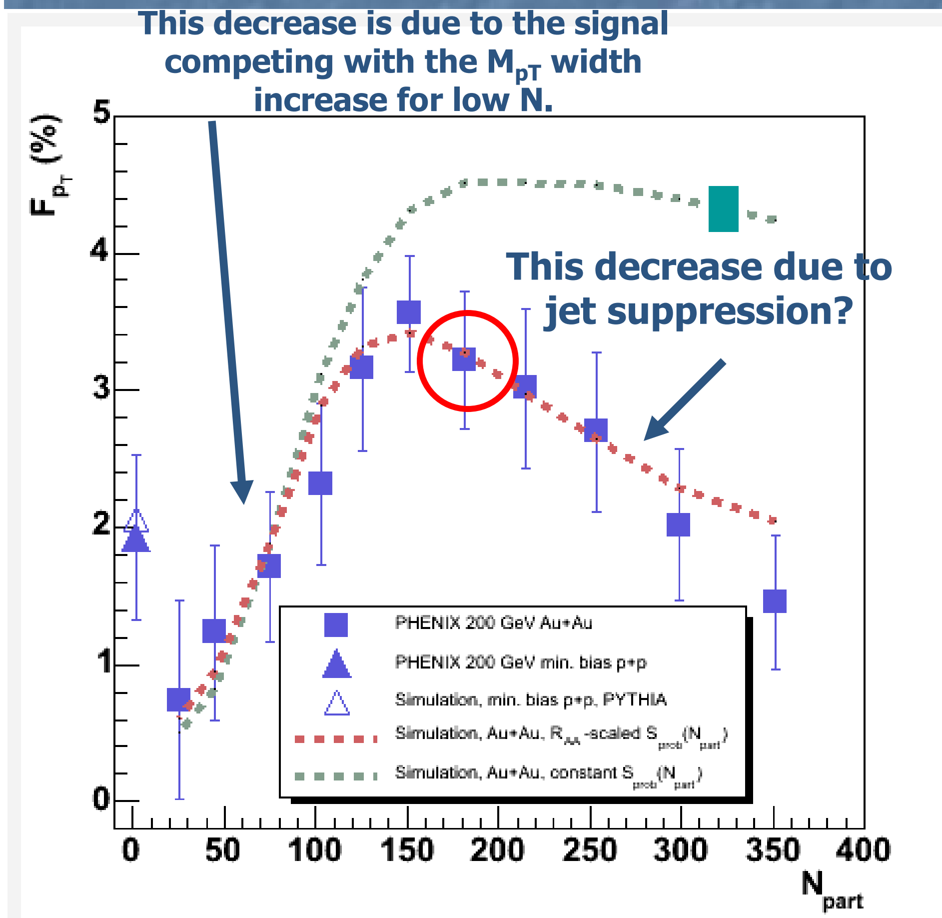

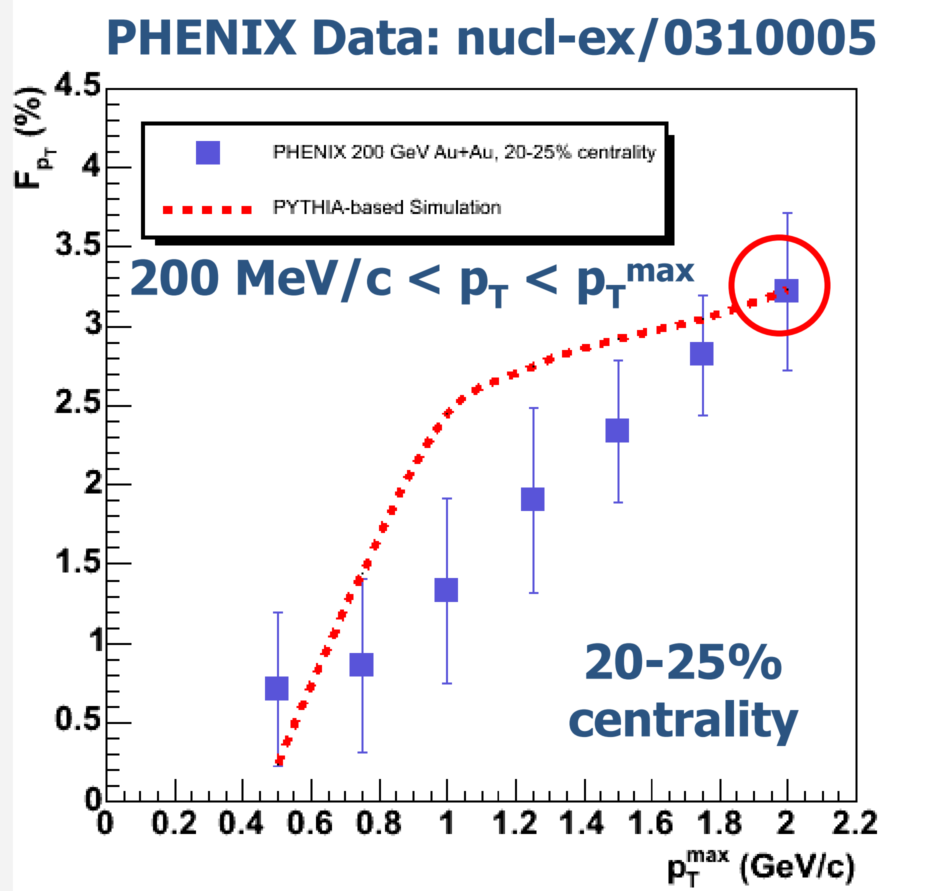

Impact Parameter Fluctuations: HIJING 1.37

Corrections for geometry fluctuations are estimated using HIJING 1.37 run a) with a fixed impact parameter, and b) with an impact parameter covering the range of the 5% centrality bin. Estimations match the 1% centrality data. Estimated systematic errors are 12-15% (included in all further data points.

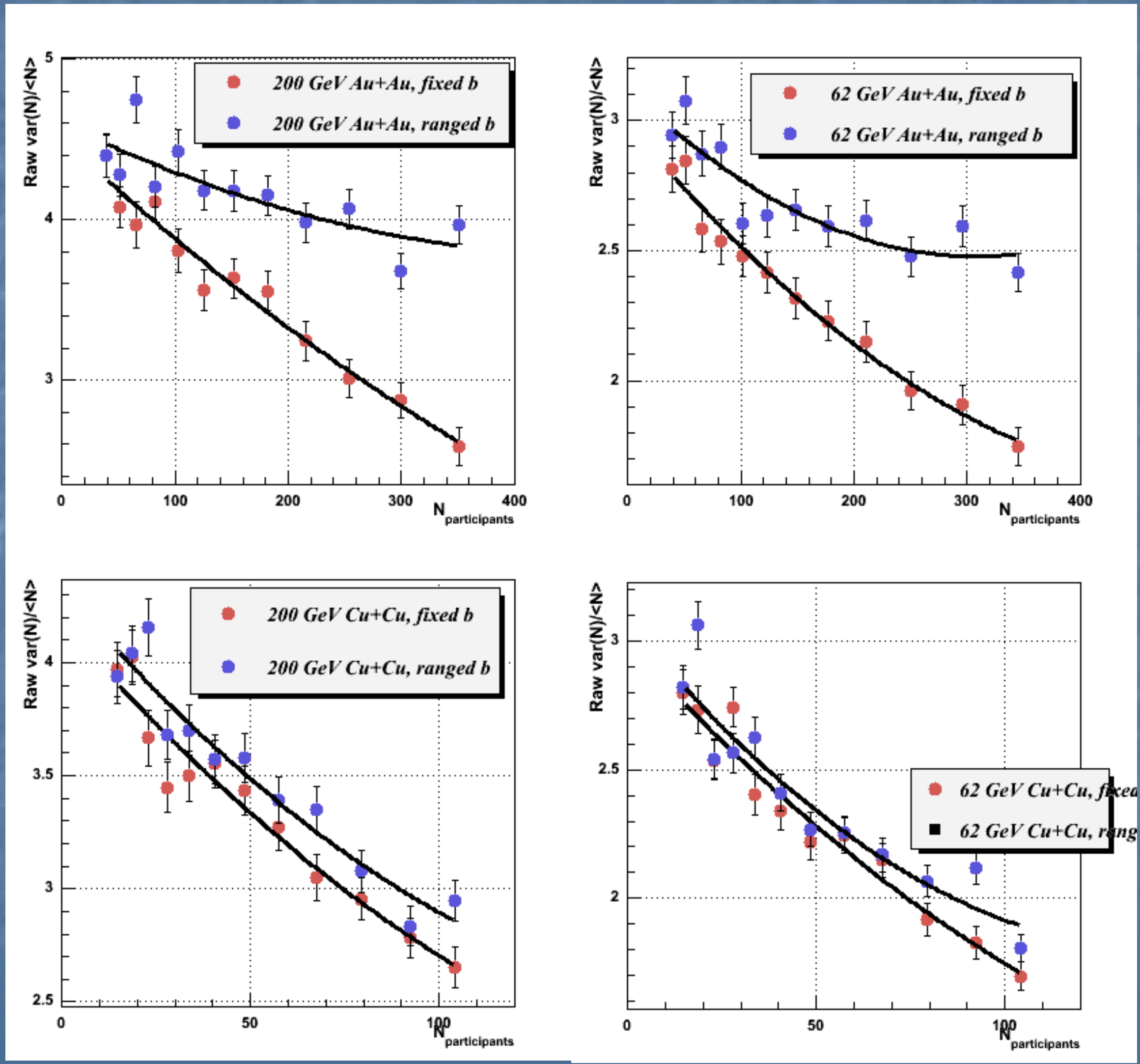

Relations to the observable N.B.D k

Two point correlation function in one dimensional case in a fixed *T*

$$G_2(|\eta_1-\eta_2|) \equiv \left\langle (\rho(\eta_1) - <\rho>)(\rho(\eta_2) - <\rho>) \right\rangle$$

$$\propto \frac{T}{A(T)} \xi(T) e^{-|\eta_1-\eta_2|/\xi(T)}, \quad \xi(T)^2 \equiv \frac{A(T)}{a_0(T-T_c)}$$

Two particle correlation function

$$\rho_1(\eta) \equiv \frac{1}{\sigma_{inel}} \frac{d\sigma}{d\eta}, \quad \rho_2(\eta_1,\eta_2) \equiv \frac{1}{\sigma_{inel}} \frac{d^2\sigma}{d\eta_1 d\eta_2}$$

$$C_2(\eta_1,\eta_2) = \rho_2(\eta_1,\eta_2) - \rho_1(\eta_1)\rho_1(\eta_2)$$

$$C_2(\eta_1,\eta_2)/\bar{\rho}_1^2 \equiv \alpha e^{-\delta\eta/\xi} + \beta$$

Fluctuation caused by centrality bin width

Relation to N.B.D. k

$$k^{-1}(\delta\eta) = \frac{<n(n-1)>}{<n>^2} - 1 = \frac{\int_0^{\delta\eta}\int_0^{\delta\eta} C_2(\eta_1,\eta_2)/\bar{\rho}_1^2 d\eta_1 d\eta_2}{\delta\eta^2}$$

$$= \frac{2\alpha\xi^2(\delta\eta/\xi - 1 + e^{-\delta\eta/\xi})}{\delta\eta^2} + \beta$$

Susceptibility

Susceptibility is defined by the response of phase for the external field.

$$\chi_k \equiv \frac{1}{Y}\left(\frac{\partial \phi_k}{\partial h}\right) = \frac{1}{Y}\left(\frac{\partial^2(\Delta F)}{\partial \phi_k^2}\right)^{-1}$$

$$= \frac{1}{a_0(T-T_c)(1+k^2\xi(T)^2)}$$

In the static limit of $k = 0$,

$$\chi_{k=0} = \frac{1}{a_0(T-T_c)} = \frac{2Y^2}{NT}\xi(T)G_2(0)$$

χ cannot be extracted separately without temperature control, but χT value can be obtained by the mean multiplicity μ and α and ξ.

$$\chi T \propto \bar{\rho}_1^2 \alpha \xi$$

Correlation Length Excitation Function

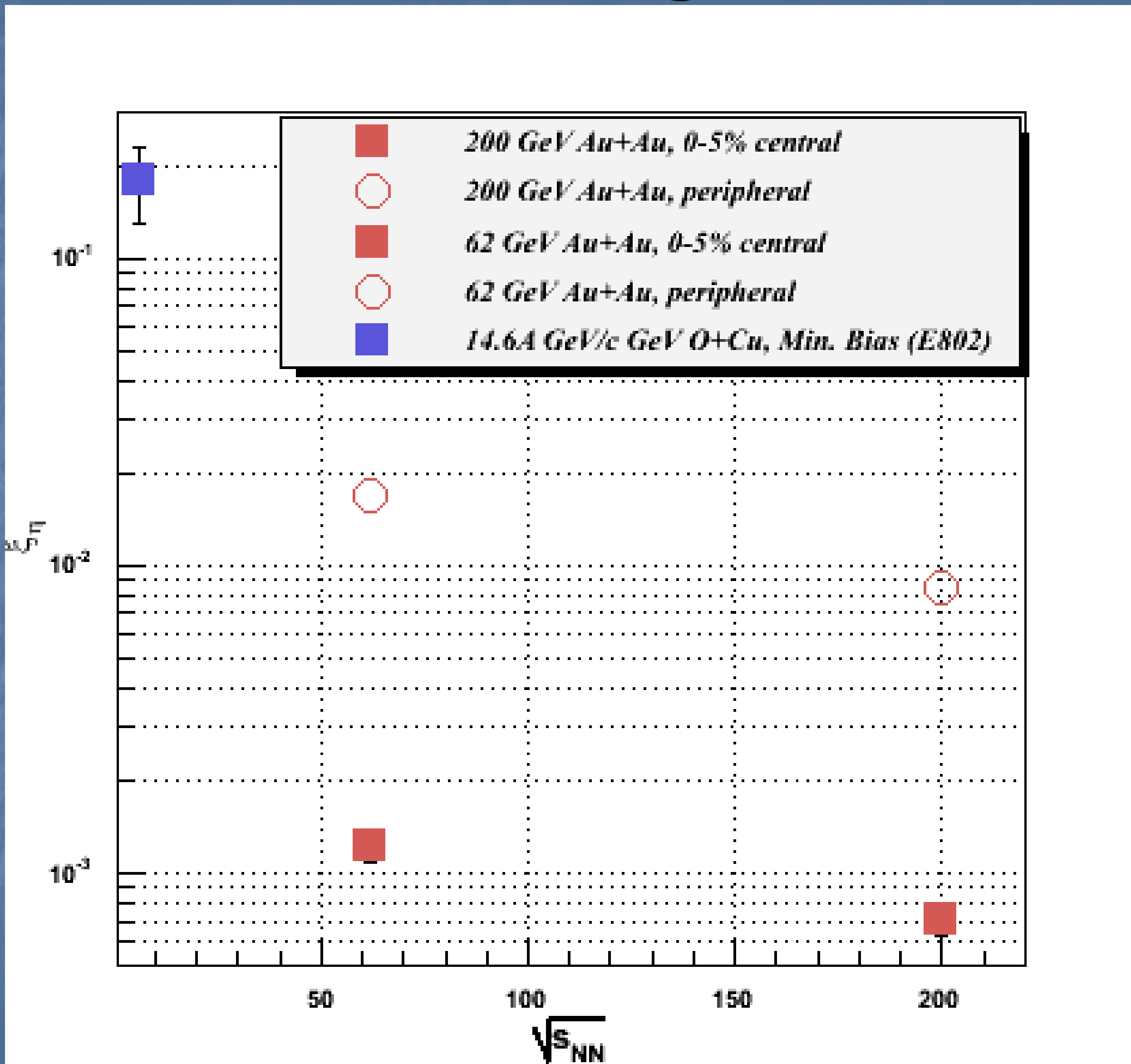

The correlation lengths measured here are small. However, they are an order of magnitude larger than the two-track resolution (when projected to the detector radius).

Near-Side Peak Width vs. Centrality

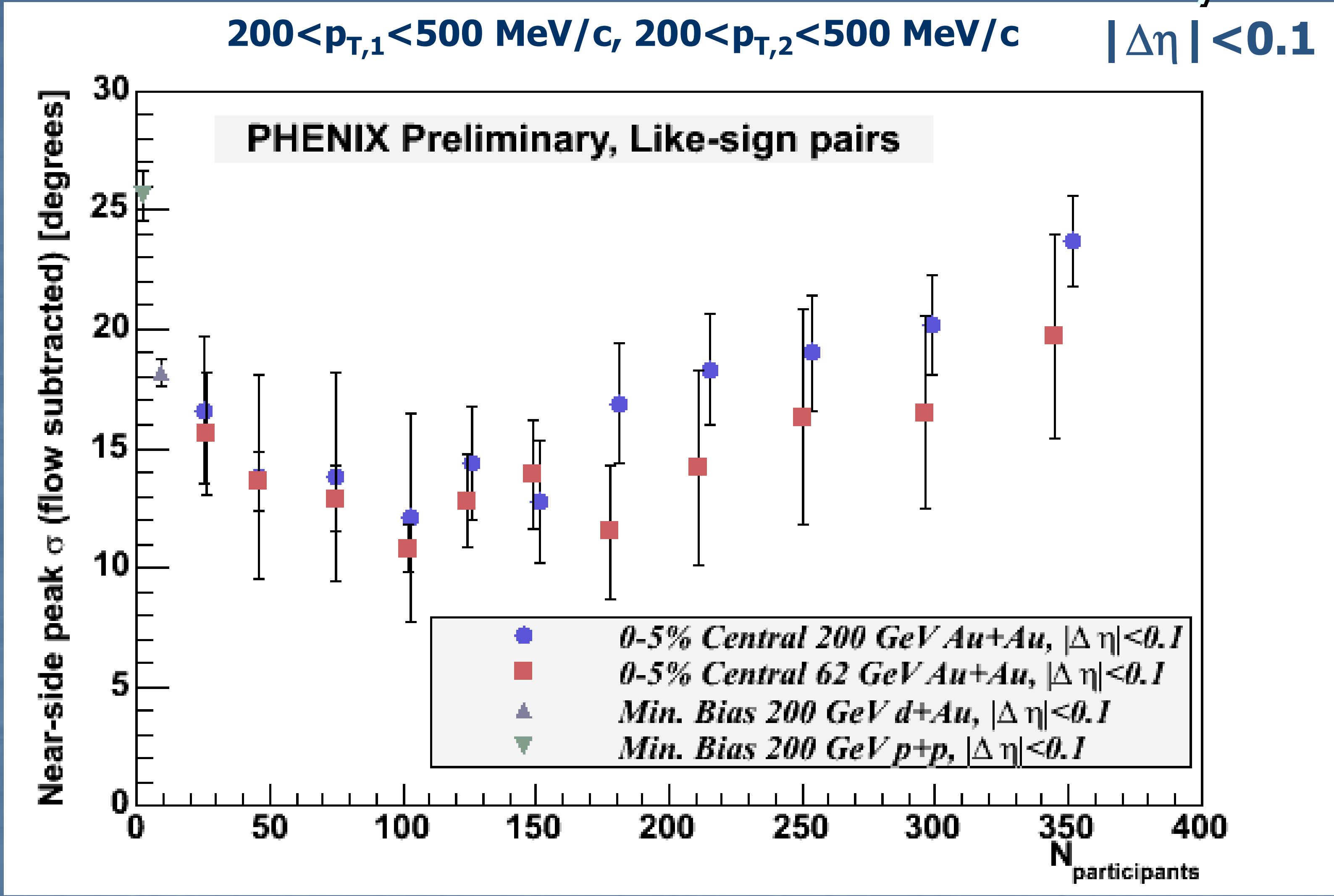

The standard deviation of the Gaussian fit to the flow- and background-subtracted near-side peaks for all like-sign pairs within the p_T range 200-500 MeV/c. The 200 GeV Au+Au peaks broaden significantly towards the most central collisions. The d+Au peak is much more narrow than the p+p peak.

Correlation Lengths: Critical Exponent Analysis

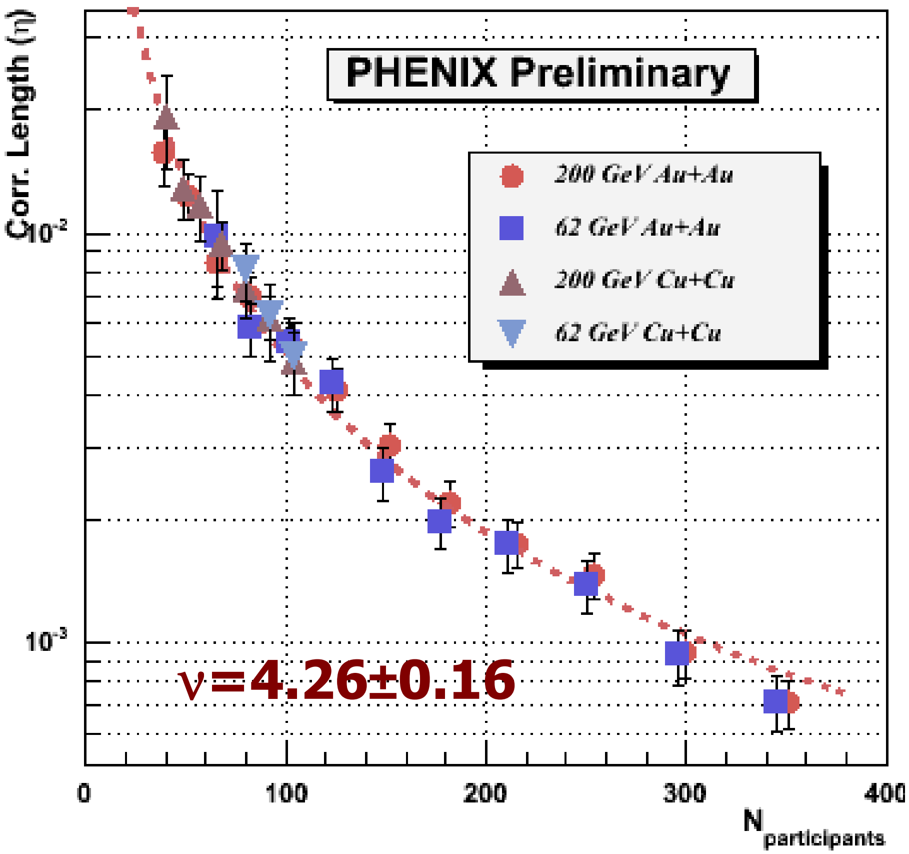

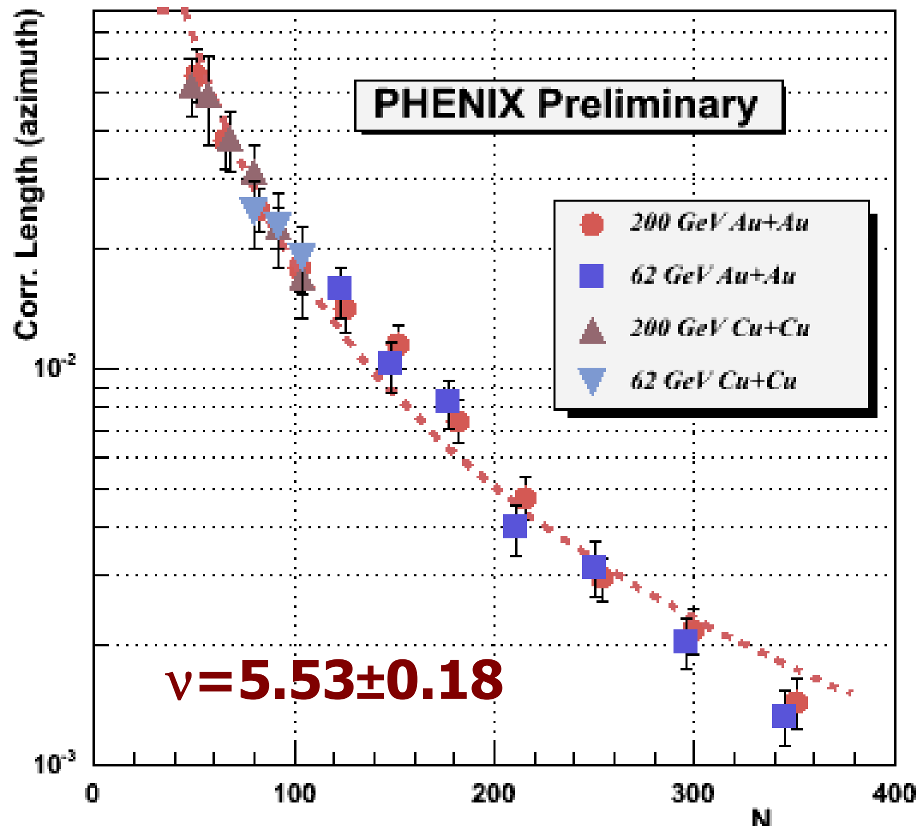

The data from other systems have bee
GeV Au+Au points for emphasis
pseudorapidity and ν=5.53 for azim
common syste

$$\xi = \left(\frac{T - T_C}{T_C} \right)^{-\nu}, T > T_C$$

Critical Exponents: p_T-independent

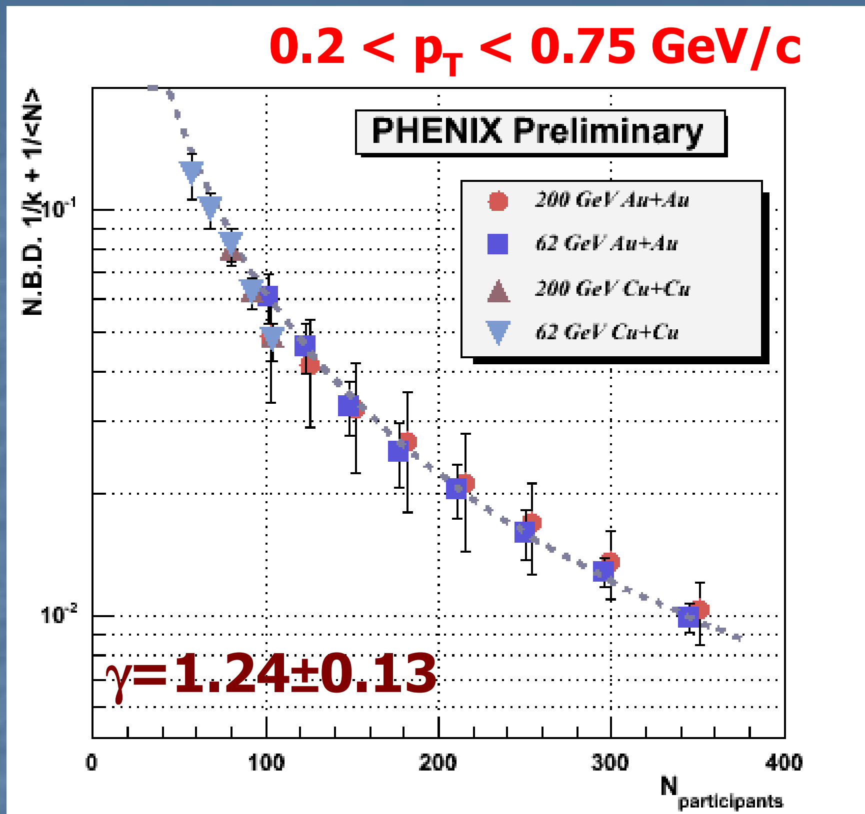

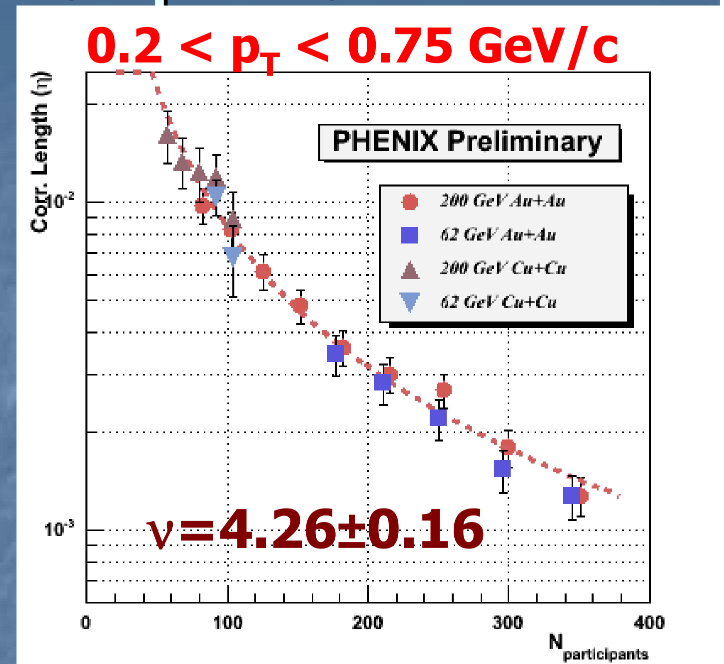

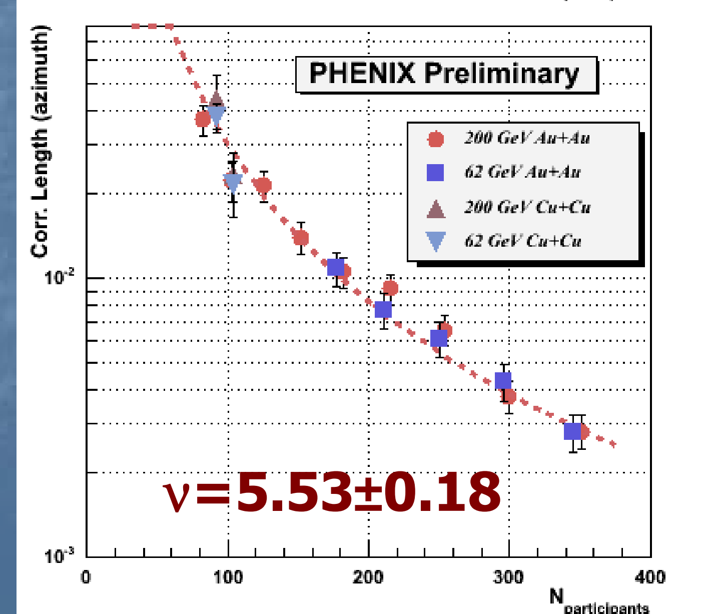

The critical exponents describing the data are independent of p_T range. The scaling appears to be driven by low p_T processes.

Thermodynamically Motivated Observables: Relating p_T Fluctuations to Heat Capacity

- **Let's switch p_T fluctuation measures to the commonly used Σ_{pt} = (event-by-event p_T variance) – (inclusive p_T variance)/(mean multiplicity per event) normalized by the inclusive mean p_T. For random particle emission, this variable is 0.**

- **From *R. Korus et al., Phys. Rev. C64 (2001) 054908*, this variable can be related to the heat capacity by:**

$$\Sigma_{p_T} = 2\sqrt{2}\left(\frac{\sqrt{\overline{\Delta p_T^2}}}{\overline{p_T}}\right)\frac{\langle T\rangle}{C_V}$$

- **The critical exponent for the heat capacity is given by:**

$$C_V = \left(\frac{T - T_C}{T_C}\right)^{-\alpha}, T > T_C$$

- **Substituting gives:**

$$\Sigma_{p_T} = A\langle T\rangle\left(\frac{\sqrt{\overline{\Delta p_T^2}}}{\overline{p_T}}\right)\left(\frac{(T - T_C)}{T_C}\right)^{\alpha}$$

<p_T> Fluctuations: Critical Exponent Analysis

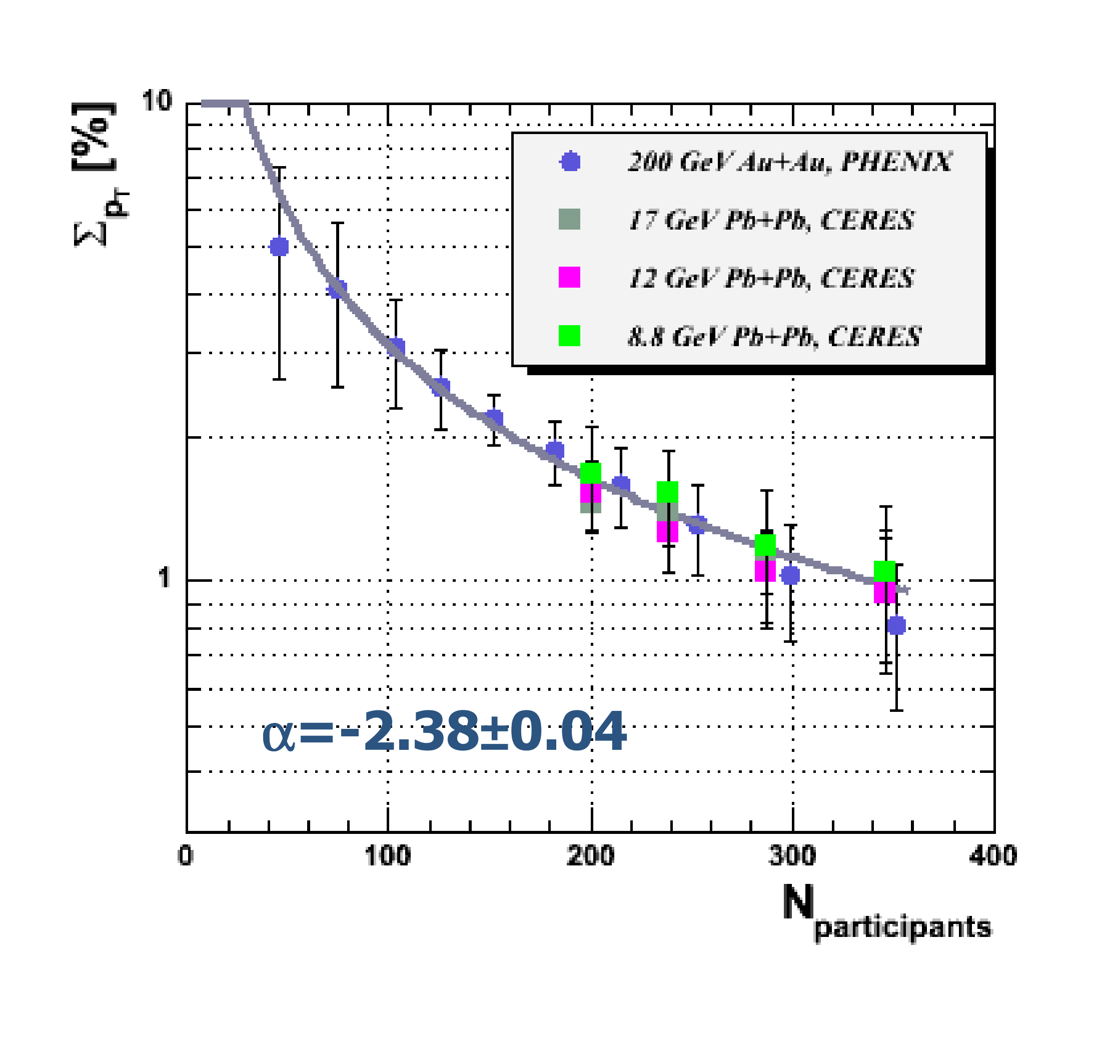

The CERES data has been scaled to the match the PHENIX data. Within the (large) errors, the various species lie on a universal curve. The fit to the PHENIX data yields α=-2.38. Typical values are α=0.1.

$<p_T>$ Fluctuations: Critical Exponent Analysis

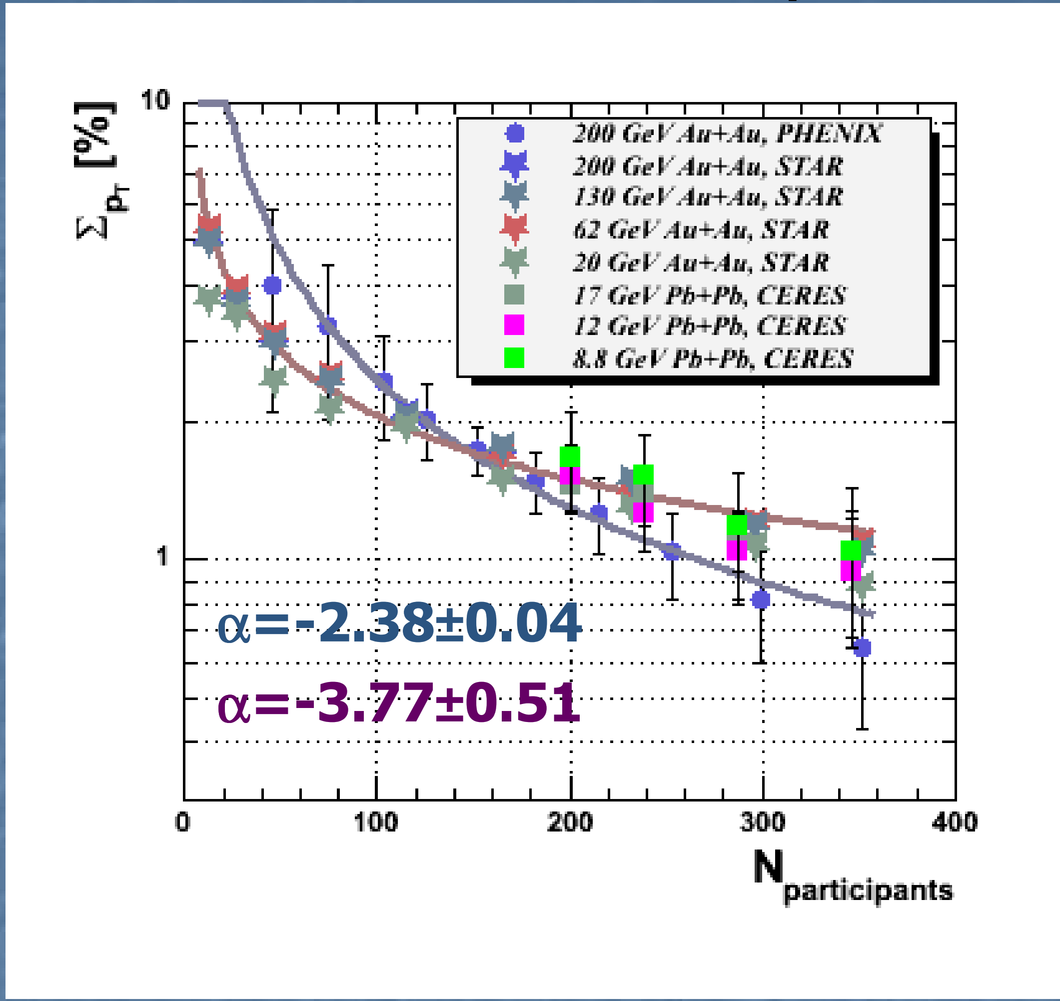

The CERES and PHENIX data has been scaled to match the STAR 200 GeV Au+Au data. Within the smaller STAR errors, the various species lie on a universal curve. The fit to the STAR data yields α=-3.77. Typical values are α=0.1.